University of New Mexico
UNM Digital Repository

Earth and Planetary Sciences ETDs | Electronic Theses and Dissertations

5-1976

The Geology Of The San Antonio Mountain Area, Tres Piedras, Taos And Rio Arriba Counties, New Mexico

Dean Eppler

Follow this and additional works at: https://digitalrepository.unm.edu/eps_etds

Part of the Geology Commons

This thesis, directed and approved by the candidate's committee, has been accepted by the Graduate Committee of The University of New Mexico in partial fulfillment of the requirements for the degree of

Master of Science

THE GEOLOGY OF THE SAN ANTONIO MOUNTAIN AREA, TRES PIEDRAS, TAOS AND RIO ARRIBA COUNTIES, NEW MEXICO

Title

Dean Eppler

Candidate

Geology

Department

Bernard Spolsky

Dean

April 19, 1976

Date

Committee

Wolfgang E. Elston

Chairman

Lee A. Woodward

Albert M. Kudo

Grant Heiken

THE GEOLOGY OF THE SAN ANTONIO MOUNTAIN AREA, TRES PIEDRAS, TAOS AND RIO ARRIBA COUNTIES, NEW MEXICO

BY

Dean Eppler

B. S., St. Lawrence University, 1974

THESIS

Submitted in Partial Fulfillment of the
Requirements for the Degree of
Master of Science

in the Graduate School of
The University of New Mexico
Albuquerque, New Mexico

May, 1976

LD
3781
N563 Ep535
cop.2

THE GEOLOGY OF THE SAN ANTONIO MOUNTAIN AREA, TRES PIEDRAS, TAOS AND RIO ARRIBA COUNTIES, NEW MEXICO

BY

Dean Eppler

ABSTRACT OF THESIS

Submitted in Partial Fulfillment of the
Requirements for the Degree of
Master of Science
in the Graduate School of
The University of New Mexico
Albuquerque, New Mexico

May, 1976

ABSTRACT

The San Antonio Mountain area is late Tertiary to early Quaternary volcanic terrane on the western edge of the San Luis Basin in the Rio Grande depression.

Calc-alkalic rocks are interlayered with flows of the Servilletta Basalt (Butler, 1946) and consist of a series of early basaltic rocks (Wissmath Craters basalt, basaltic andesites of Los Cerritos de la Cruz, Red Hill, Malette Creek), intermediate age basaltic andesite, andesite and latite of the San Antonio Mountain Volcanic Complex and late basalt of the Piñabetoso Peaks.

Data suggest that the volcanic rocks of the San Antonio Mountain area evolved from two magmas. One originated at shallow depth in a mantle bulge beneath the Rio Grande Depression and was erupted as the Servilletta Basalt (Lipman, 1969). This unit is olivine tholeiite and is widespread throughout the San Luis Basin. The second magma was calc-alkalic. Three separate magmas were segregated from the parent magma and emplaced beneath the field area at different times and location. One of the magmas was erupted as the early basalt and basaltic andesites. Evolution of the second magma formed the early andesite and latite of the San Antonio Mountain Volcanic Complex. The third magma was erupted as the late basaltic andesite and andesite of San Antonio Mountain. The chemical evolution of these magmas may have been the result of fractionation or crustal contamination. The basalt of Piñabetoso

Peaks appears to be only slightly differentiated and may have been derived directly from the original parent magma or from a different source magma.

The volcanos of the field area can be classified in four groups, based on shape and internal structure. Tholeiite shield volcanos (Wissmath Craters) were constructed of thin lava flows dipping at low angles away from the vent. Cinder and lava cones (north and south Piñabetoso Peaks) consist of cinders and spatter which have been intruded by later lavas. The intrusions dip toward a central vent which is also probably the source of the pyroclastics. Lava cones (north and south Cerritos de la Cruz, Red Hill) consist of lava flows which have piled up around a central vent and have steep, quaquaversal dips. Some lava cones, however, have flows which dip toward the vent as well as away. These volcanos are often breached by later explosions. Flow domes (San Antonio Mountain) are constructed of thick lava flows which have been erupted from a central vent and have piled up around the vent to form a steep, domical structure. These flows have steep, quaquaversal dips. Pyroclastic activity also forms hills of agglomerate around the central vent.

Correlation of external shape with bulk chemistry indicates that for large structures, such as shields and flow domes, composition of the lava flows is the major factor in determining the shape of the volcano. With increasing silica content, flows are thicker, more viscous and travel for shorter distances from the vent, forming steep sided structures. For these volcanos eruptive history does not appear to greatly affect the final shape of the volcano. In smaller structures, such as lava cones, eruptive history and vent conditions during eruption appear to be more significant than bulk chemistry in determining the shape of the volcano.

TABLE OF CONTENTS

LIST OF FIGURES

TABLES

INTRODUCTION

Location

The San Antonio Mountain field area is located along the boundary of Taos and Rio Arriba counties, approximately 64 km (40 mi) northwest of Taos, New Mexico (Fig. 2). It covers 390 km^2 (156 mi^2) within the Los Pinos, Piñabetoso Peaks, San Antonio Mountain and La Segita Peaks 7-1/2 minute quadrangles.

Geologic Setting

The San Antonio Mountain area is located in the Rio Grande depression on the southwestern edge of the San Luis Basin (Fig. 2). Bryan (1938) described the depression as a series of en-echelon basins which extend north from El Paso, Texas through central New Mexico into southern Colorado. The San Luis Basin is the northernmost of these. The initial rifting which formed the depression began in late Miocene time (Chapin, 1971) and has resulted in approximately 10,340 m (36,000 ft) of structural relief on the east side of the San Luis Basin.

Volcanism has become an increasingly important process in the basin during the last 5 m.y., when as much as 980 m (1,500 ft) of basalt of the Servilletta Formation (Butler, 1946; Montgomery, 1953) formed the Taos Plateau. The majority of the rocks within the map area have erupted on to basalt flows of the Servilletta Formation.

The Brazos uplift is west of the San Antonio Mountain area and forms the western boundary of the San Luis Basin. The uplift

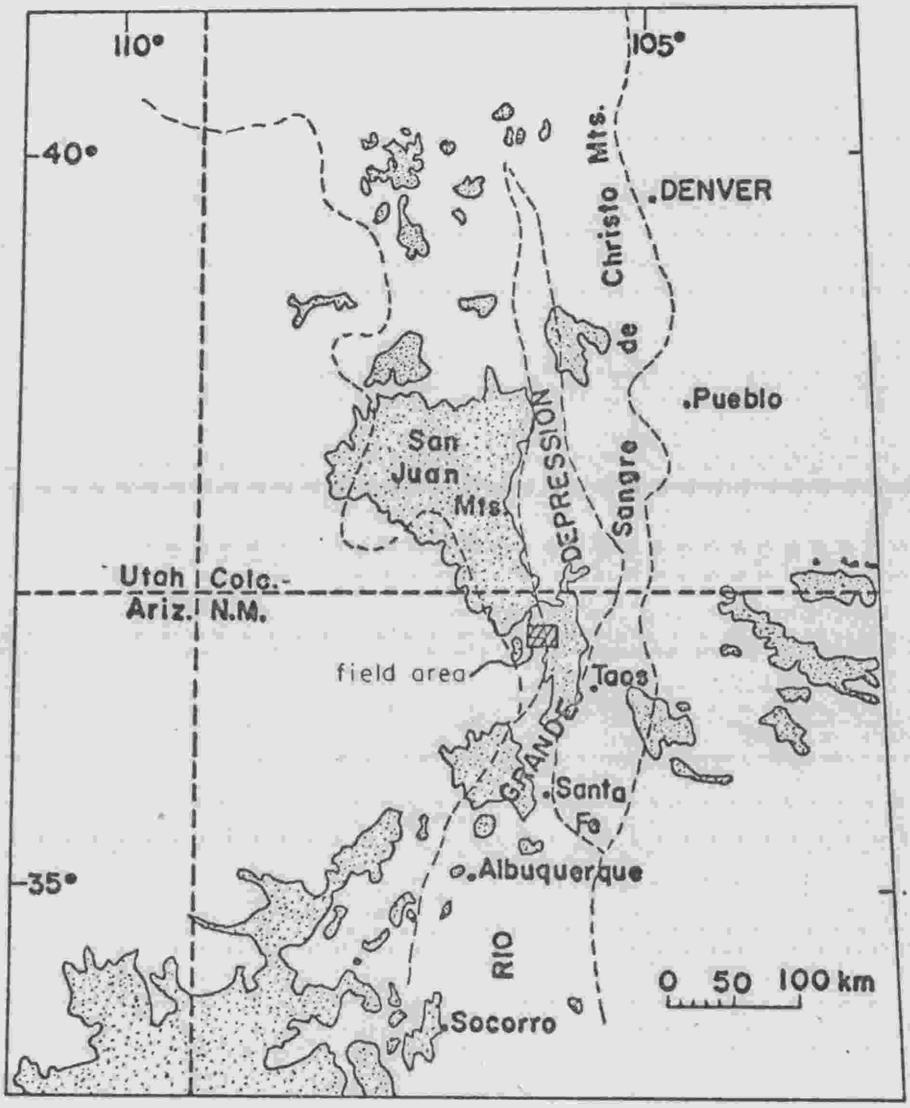

Figure 2. Location map and geologic setting of the San Antonio Mountain field area. Light stiple indicate Cenozoic volcanic rocks. After Lipman and Mehnert (1975).

consists of Precambrian schist, granitic gneiss and pegmatite, and quartzite which are overlain by Pliocene volcanic rocks erupted from the San Juan volcanic center to the northwest (Kelley, 1956; Muehlberger, 1968).

Previous Work

Earlier studies of the northern Rio Grande Rift in the vicinity of San Antonio Mountain have been concerned with general geology or detailed petrologic and geophysical investigations. Butler (1946, 1971) mapped approximately 1625 km^2 (650 mi^2) of the eastern Tusas Mountains and the western Taos Plateau, including portions of the San Antonio area. He subdivided the rocks in the field area into four units: the lower and upper basalt members of the Hinsdale Formation; quartz latite flows of San Antonio Mountain; and volcanic rocks and gravels of the Servilletta Formation. Lambert (1966) and Bingler (1968) drew primarily on the work of Butler (1946) in discussing the volcanic geology of the Tusas-Tres Piedras, N.M., area. Aoki (1967), Lipman (1969) and Lipman and Mehnert (1975) have studied the petrology of alkali basalts and the olivine tholeiites of the Servilletta Formation as they relate to the structural development of the Rio Grande depression. In addition, Ozima and others (1967) have done paleomagnetic work and K-Ar age dating of samples from the Rio Grande Gorge.

Acknowledgments

I wish to thank my advisor, Wolfgang E. Elston, and the other members of my committee, Albert M. Kudo and Lee A. Woodward of the University of New Mexico, and Grant Heiken and Thomas R. McGetchin of Los Alamos Scientific Laboratories. Their guidance during field and laboratory work and during the preparation of the manuscript greatly improved this thesis. Many hours of stimulating discussions with K. N. Loeber and L. S. Crumpler also were extremely beneficial. Mr. Bobby Carey of Tres Piedras, N.M. kindly provided lodging as well as access to his land. M. E. Register and J. W. Husler provided chemical analyses with great speed and accuracy. T. J. Bornhorst provided and ran the computer program which calculated norms and theoretical viscosities. J. S. Wadell provided much needed guidance on the intracacies of the International Code of Stratigraphic Nomenclature.

STRATIGRAPHY AND PETROGRAPHY

General Statement

Field relations indicate that all of the rocks within the San Antonio Mountain area are late Tertiary to Quaternary in age. K-Ar age determinations (P. W. Lipman, personal communication, 1975) on selected units have provided an absolute age framework which has confirmed the stratigraphic relationships determined in the field.

Uncertainty over the absolute age of the Tertiary-Quaternary boundary (Funnel, 1964) prompted the adoption of a broad stratigraphic boundary ranging from approximately 3.5-1.5 m.y. Rock stratigraphic units erupted during this interval were mapped as transitional between the Tertiary and the Quaternary.

A summary of modal analyses for all thin sections is given in Table 1.

Tertiary Rock Units

Basalt of Wissmath Craters

The basalt of Wissmath Craters forms the shield volcano in the southeastern quadrant of the field area. The unit can be divided into three members, based on chemistry and petrography: a xenocrystic tholeiite member, an olivine tholeiite member and a xenocrystic alkali basalt member.

Xenocrystic Tholeiite Member. The xenocrystic tholeiite member is the most widespread of the three members. The unit is massive,

Table 1. Modal percentages of samples from the San Antonio Mountain field area. P indicates that the mineral occurs as a phenocryst; G indicates groundmass grains.

	1	2	3	4	5	6	7	8
Augite	P 15	P, G 7	G 10-21	G 11-24	P 40	P, G 18	P 18	P, G 4-5
Hypersthene					P Tr	P 4	P 1	P, G 1
Olivine	P 7	P 4	G 2	P 2	P Tr	P Tr	P Tr	P Tr
Plagioclase	G 37	P, G 37	P, G 22-53	P 45-56	P 46	G 72	P,G 45	P, G 20-44
Opaques	G 6	G 52	G Tr-3	G 2-4	G 15	G 5	G 5	G 3
Plagioclase megacrysts			1-6				Tr	
Xenocrysts	Tr		Tr		Tr		Tr	
Mesostasis	40		6-28	6-14			32	16-41
Texture	Intergranular porphyritic vesicular	Intergranular porphyritic	Intersertal with brown glass	Diktytaxitic poikilitic	Diktytaxitic	Intergranular vesicular	Intergranular	Intergranular vesicular

1- Wissmath Craters Basalt xenocrystic tholeiite member
2- Wissmath Craters Basalt olivine tholeiite member
3- Wissmath Craters Basalt alkali basalt member
4- Servilleta Basalt
5- Malette Creek basaltic andesite
6- Red Hill basaltic andesite
7- Los Cerritos de la Cruz basaltic andesite
8- San Antonio Mountain volcanic complex first lower andesite member

Table 1 continued. Modal percentages of samples from the San Antonio Mountain field area.

	9		10		11		12		13	
Augite	P,G	11	G	Tr-8	P,G	12	G	3-3	P,G	15
Hypersthene	P,G	4	P	1-5	G	1	P,G	Tr-3	P	1
Olivine									P	2
Plagioclase	P,G	57	G	32-91	P,G.	73	G	29-66	P,G	69
Opaques	G	4	G	1-8	G	8	G	2-4	G	13
Plagioclase megacrysts						Tr		Tr		Tr
Xenocrysts						5				
Mesostasis		24		11-55				14-35		
Texture	Intersertal with black glass vesicular		Porphyritic		Porphyritic		Intersertal with brown glass vesicular		Flow-banded intergranular porphyritic	

9- San Antonio Mountain second lower andesite member
10- San Antonio Mountain latite member
11- San Antonio Mountain upper basaltic andesite member
12- San Antonio Mountain upper andesite member
13- Pinabetoso Peaks basalt

Table 2. Estimated physical parameters of volcanic rocks. Units in stratigraphic order.

		estimated exposure	estimated thickness	estimated volume
SAN ANTONIO MOUNTAIN VOLCANIC COMPLEX	Pinabetoso Peaks basalt	18 km^2	<16m	0.3 km^3
	Upper andesite member	6.4 km^2	<60m	3.8 km^3
	Cinder cone member	<6.4 km^2	unknown	unknown
	Upper basaltic andesite member	15 km^2	<22m	.3 km^3
	Latite agglomerate member	<.64 km^2	unknown	unknown
	Latite flow member	35 km^2	unknown	unknown
	Second lower andesite member	<0.6 km^2	unknown	unknown
	First lower andesite member	<6.4 km^2	unknown	unknown
	Red Hill basaltic andesite	3.8 km^2	<12m	.05 km^3
	Los Cerritos de la Cruz basaltic andesite	20 km^2	<24m	0.4 km^3
	Malette Creek basaltic andesite	5.1 km^2	31m	0.2 km^3
	Servilletta Basalt	127 km^2	≥37m	≥4.7 km^3
WISSMATH CRATERS BASALT	Alkali basalt member	<0.64 km^2	unknown	unknown
	Olivine tholeiite member	26 km^2	18m	0.5 km^3
	Xenocrystic tholeiite member	51 km^2	300m	15.3 km^3

dark grey to black with numerous quartz xenocrysts and pitted plagioclase megacrysts. Microscopically, plagioclase phenocrysts are set in a groundmass of plagioclase, olivine, augite, and opaque minerals. Plagioclase phenocrysts are approximately 0.3-2.0 mm in size, subhedral to anhedral and optically zoned. Groundmass grains are subhedral to anhedral and ~0.5 mm in size. Plagioclase megacrysts range in size from ~1.0 - 6.0 mm and are vesicular and rounded, showing evidence of incipient resorption (Fig. 5). Quartz xenocrysts are rounded and range from approximately 1.0-2.5 mm. Individual xenocrysts commonly have a thin rim of pyroxene (Fig. 4).

Olivine Tholeiite Member. The rock is black and sparsely vesicular, with small olivine phenocrysts set in an aphanitic groundmass. Thin sections of the unit consist of phenocrysts of plagioclase, olivine and augite set in a groundmass of augite, plagioclase and opaque minerals. Augite and olivine phenocrysts are 0.1-0.3 mm wide, while plagioclase phenocrysts are 0.3-1.5 mm long. Groundmass grains are <0.1 mm wide. Many olivine grains are rimmed by magnetite grains, possibly indicating some reaction of olivine with the melt (Fig. 5).

Xenocrystic Alkali Basalt Member. Individual fragments of agglomerate are scoriaceous to massive, black, with numerous rounded quartz xenocrysts and fused sediments (Fig. 6). Phenocrysts of olivine and augite are set in an intersertal groundmass of plagioclase microlites, opaque minerals and brown glass.

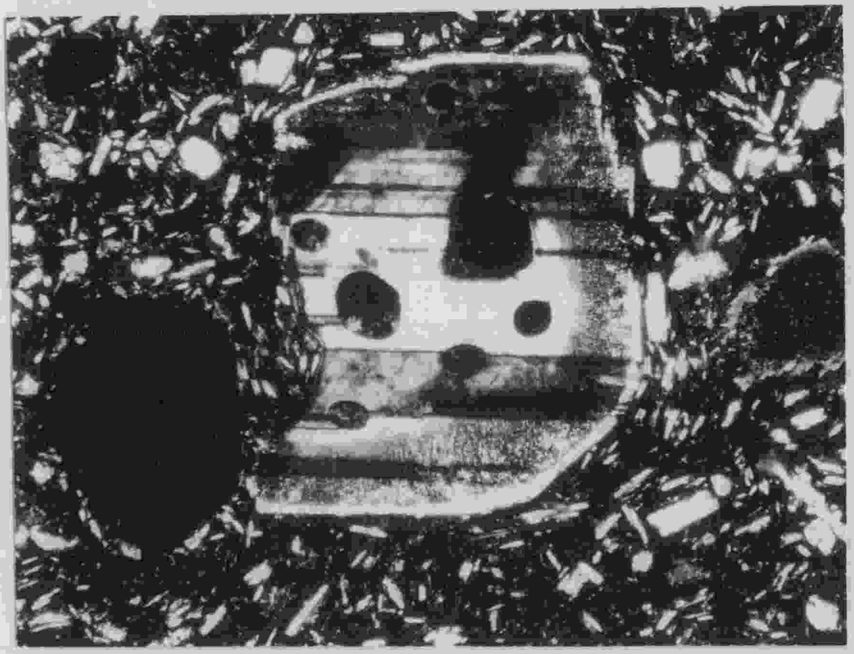

Figure 3. Plagioclase megacryst in a sample from the xenocrystic tholeiite member of the Wissmath Craters Basalt. Note the numerous vesicles within the megacryst and the thin rim of newly crystallized plagioclase, indicating resorption and re-equilibration. Scale bar - 1 mm.

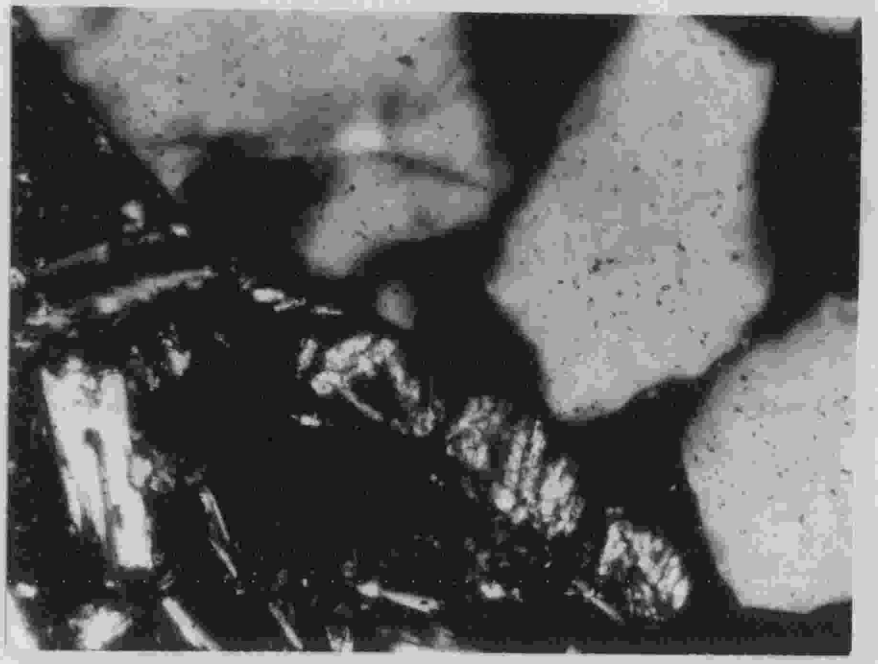

Figure 4. Quartz xenocryst in a sample of the xenocrystic tholeiite member of the Wissmath Craters Basalt. Note thin reaction rim of pyroxene. Scale bar - 0.2 mm.

Figure 5. Olivine grain with a magnetite reaction rim in a sample of the olivine tholeiite member of the Wissmath Craters Basalt. Scale bar - 0.2 mm.

Phenocrysts are subhedral to euhedral and are often skeletal, and range from 0.1 to 1.5 mm. Groundmass grains are subhedral to euhedral and are <0.1 mm.

Gravel

The gravel unit is exposed over the southwestern border of the field area and is probably equivalent to the undivided part of the Los Piños Formation of Butler (1946). The total exposure of the unit is <6.4 km^2 (2.5 mi^2) and its total thickness is unknown. The gravel consists of loosely consolidated, interbedded silt, sand and cobbles of varying lithology, including Tertiary andesite and felsite from the San Juan Mountains, and Precambrian granitic pegmatite.

Basalt of the Servilletta Formation of Butler (1946, unpub., Montgomery, 1953)

The Servilletta Formation was named by Butler (1946) for exposures of alluvial gravels interlayered with basalt flows on the Taos Plateau. The formation is exposed over the eastern, northern, and western portions of the field area. The rock is diktytaxitic, black to dark grey and coarsely porphyritic, with phenocrysts of plagioclase and olivine in an aphanitic groundmass. In thin section, phenocrysts of plagioclase and olivine are poikilitically enclosed in augite, with an interstitial mesostasis of augite, plagioclase and opaque minerals. Plagioclase phenocrysts are subhedral to anhedral and are 01.-0.3 mm. Augite grains are anhedral and range from 0.1 to 1.2 mm. Mesostasis grains are anhedral and are <0.1 mm.

Figure 6. Inclusion of fused sediments in a sample of agglomerate from the xenocrystic alkali basalt member of the Wissmath Craters Basalt.

Ozima *et al.* (1967) has dated samples of the Servilletta Basalt from the Rio Grande Gorge at 3.6-4.5 m.y. Lipman and Mehnert (personal communication, 1975) have dated two samples of Servilletta basalts at 3.45 ± 1.48 m.y. and 3.66 ± 0.77 m.y.

Basaltic Andesite of Malette Creek

The basaltic andesite of Malette Creek is exposed over the southern edge of the area, south of Malette Creek (Fig. 1). The unit thins rapidly to the southwest. The rock is vesicular, grey, medium grained and porphyritic, with phenocrysts of olivine and plagioclase set in an aphanitic groundmass. In thin section, phenocrysts of plagioclase, hypersthene, augite and olivine are set in a groundmass of opaque minerals and augite. Sparse xenocrysts of quartz rimmed by pyroxene are also present. Olivine phenocrysts are euhedral to subhedral and range from 0.2-2.4 mm. Augite and hypersthene phenocrysts are 0.3-0.6 mm and are subhedral to anhedral. Plagioclase phenocrysts are 0.1-1.5 mm and are subhedral. Groundmass grains are euhedral to anhedral and are <0.1 mm. Quartz xenocrysts are rounded and are 1.5 mm.

Tertiary-Quaternary Rock Units

Basaltic Andesite of Los Cerritos de la Cruz

The basaltic andesite of Los Cerritos de la Cruz is exposed southwest of San Antonio Mountain and forms the lava cones of Los Cerritos de la Cruz. The unit consist of three roughly contemporaneous units which have identical petrography. The basal unit was probably erupted from a fissure over which the later lava cones were built. The remaining two units form, respectively, the northern and southern cones of the cerritos. Hand specimens are massive and black, with numerous quartz xenocrysts. The rock has as intergranular texture, with phenocrysts of olivine, megacrysts of plagioclase and xenocrysts of quartz in a very-fine-grained groundmass of plagioclase augite, opaque minerals and interstitial glass. Phenocrysts of olivine are ~1.0 mm and are euhedral to subhedral. Plagioclase megacrysts are 0.6-2.4 mm and are vesiculated and rounded, suggesting partial resorption. Quartz xenocrysts are rounded, 0.6-2.0 mm and rimmed by pyroxene. Groundmass grains are subhedral to anhedral and are <0.5 mm.

Basaltic Andesite of Red Hill

The basaltic andesite of Red Hill forms the lava cone and associated flows along the southern boundary of the field area. The rock is massive dark grey, aphanitic and weathers to a dark red. Thin sections have phenocrysts of hypersthene, augite, and olivine in a vesicular groundmass of intergranular plagioclase and augite. The phenocrysts are euhedral to subhedral and range in size from 0.2-0.6 mm and are partially to completely rimmed with opaque minerals. Groundmass grains are <0.1 mm and are subhedral to euhedral.

San Antonio Mountain Volcanic Complex

The San Antonio Mountain Volcanic Complex is an intermediate volcanic vent which was active for ~1 m.y. during the late Tertiary and early Quaternary. The total exposure of the complex is ~51 km^2 (20 mi^2) and it has an estimated volume of 14.0 km^3. The complex can be divided into seven members: first lower andesite member, second lower andesite member, latite flow member, latite agglomerate member, upper basaltic andesite member, cinder cone member and upper andesite member.

First Lower Andesite Member. The first lower andesite member forms small, discontinuous outcrops south and southeast of San Antonio Mountain. The andesite is vesicular to scoriaceous, black, with sparse phenocrysts of altered olivine set in an aphanitic groundmass. Rare outcrops exhibit well developed pahoehoe structure (Fig. 8) indicating a high temperature of eruption (MacDonald, 1953). In thin section, phenocrysts of olivine, plagioclase, hypersthene and augite are set in an intersertal to intergranular groundmass of augite, hypersthene, plagioclase opaque minerals and black glass. Olivine phenocrysts are 0.4-0.1 mm, subhedral to euhedral and rimmed with pyroxene, possibly indicating a reaction with the melt (Fig. 8). Plagioclase phenocrysts are 0.1-1.0 mm and are euhedral to subhedral. Augite and hypersthene phenocrysts are 0.1-0.6 mm and are euhedral to subhedral. Groundmass grains are <0.01 mm and are subhedral to anhedral.

Second Lower Andesite Member. The second lower andesite member forms one small flow on the south side of San Antonio Mountain (Fig. 1) which has been overlain by later latite flows. Hand specimens are vesicular, dark grey and aphanitic. In thin

Figure 7. Pahoehoe structure on the surface of an outcrop of the first lower andesite member of the San Antonio Mountain volcanic complex.

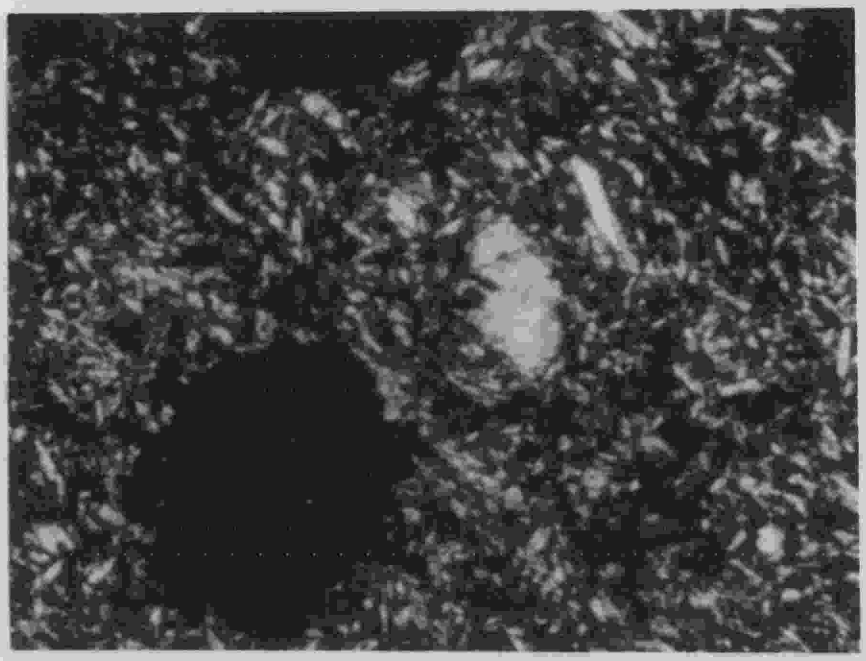

Figure 8. Olivine grain with a pyroxene reaction rim in the first lower andesite member. Scale bar = 0.2 mm.

section, phenocrysts of hypersthene, augite and plagioclase grade in size into an intersertal groundmass of hypersthene, plagioclase, augite, opaque minerals and black glass. Plagioclase grains are euhedral to subhedral and are ~0.6 mm. Hypersthene grains range from 0.05-0.5 mm and are euhedral to subhedral. Opaque minerals are ~0.1 mm and are subhedral to anhedral.

Latite Flow Member. The latite flow member is exposed over ~35 km^2 (14 mi^2) of San Antonio Mountain. Megascopic features visible in the field allow differentiation of the member into four subunits: (1) a black, microcrystalline, massive sub-unit which has sparse hypersthene phenocrysts, (2) a silver to grey, platy massive sub-unit, (3) a silver, holocrystalline vesicular sub-unit which weathers to a brick red color, and (4) a black, holocrystalline, vesicular to scoriaceous sub-unit. Although these units are rarely seen in contact, a possible relationship between them can be hypothesized on the basis of field relations (Fig. 9). In addition to the four subunits, two varieties of breccia have been delineated: an intra flow breccia, derived apparently from internal shearing in a partially solidified flow, and an interflow breccia, formed when a late flow is erupted onto the rubbly upper surface of an earlier flow, annealing the upper surface of rubble (Fig. 11).

In thin section, the four subunits are almost indistinguishable. The most significant differences are the modal percentage of glass and the size of the phenocrysts. Phenocrysts of hypersthene, augite and plagioclase are set in an intergranular to intersertal groundmass of hypersthene, augite, plagioclase, opaque minerals and brown glass. In most cases, there is no orientation of the plagioclase laths in the groundmass, but sparse samples are subtrachytic to trachytic. Hypersthene phenocrysts are dominantly euhedral and range from 0.01-1.0 mm. Plagioclase and augite phenocrysts are euhedral to subhedral and range from ~0.05-~0.5 mm, and often grade into groundmass grains. Groundmass grains are subhedral to anhedral and are <0.02 mm.

The latite flow member has been dated by the K-Ar method at 3.04 ± 0.17 m.y. (P.W. Lipman, personal communication, 1975).

Latite Agglomerate Member. The latite agglomerate member forms a small pile of agglomerate on the summit of Antone Peak and is the only evidence of a vent on the mountain. In hand specimen, the rock consists of angular fragments of black, glassy latite in a red matrix. Thin sections show the matrix to be <0.1 mm plagioclase microlites in a mesostasis of red glass.

Upper Basaltic Andesite Member. The upper basaltic andesite member forms the large flow which extends northeastward from the northern flank of San Antonio Mountain. Hand specimens are vesicular to massive, dark grey and aphanitic with sparse xenocrysts. The basaltic andesite has phenocrysts of plagioclase, augite and hypersthene, sparse xenocrysts of quartz and megacrysts of plagioclase are set in a groundmass of plagioclase, augite, hypersthene and opaque minerals. Plagioclase megacrysts are

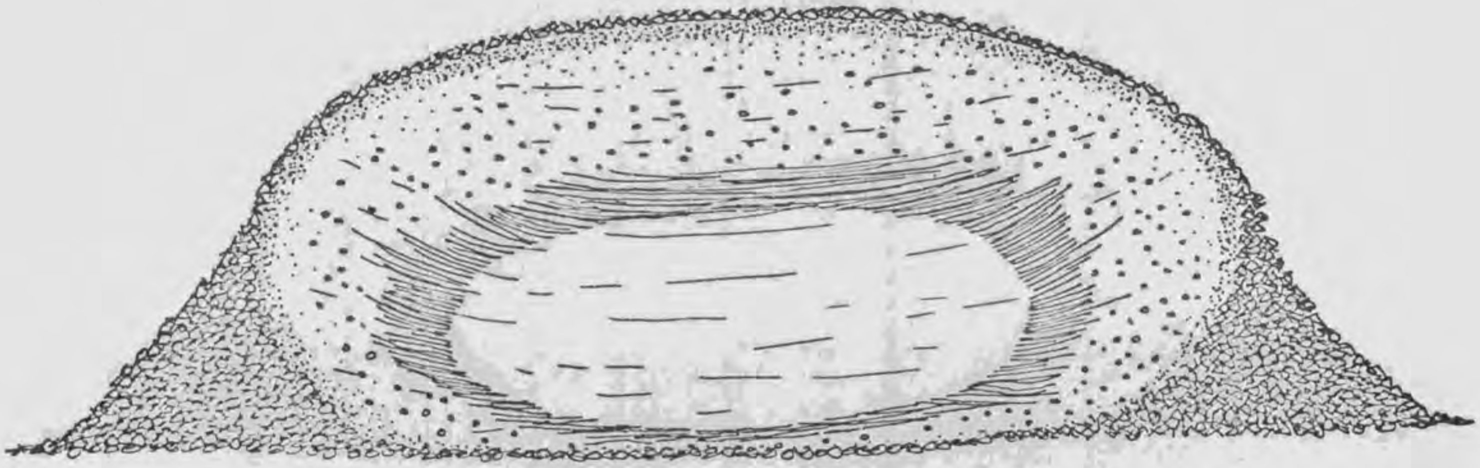

Figure 9. Schematic transverse cross section of a typical latite flow showing the occurrence of the sub-units. Lines in the interior of the flow represent joints.

Figure 10a. Intra-flow breccia.

Figure 10b. Inter-flow breccia.

~1 mm, rounded and vesiculated, indicating some partial resorption. Quartz xenocrysts are 1.0-4.5 mm in diameter, rounded, and have <0.05 mm thick reaction rims of pyroxene. Augite and hypersthene phenocrysts are 0.3-0.5 mm and are subhedral to anhedral. Groundmass grains are <0.1 mm and anhedral to euhedral.

The upper basaltic andesite has been dated by the K-Ar method at 2.19 ± 0.15 m.y. (P.W. Lipman, personal communication, 1975).

Cinder Cone Member. The cinder cone member forms a small cinder cone northeast of San Antonio Mountain which as been partially engulfed by andesite flows. The cone consists of light grey to red ash, lapilli and blocks up to 50 cm in size, which are poorly sorted and crudely stratified. Individual blocks have sparse xenocrysts of quartz and fused sediments. The probable composition of the pyroclastic unit is basaltic andesite.

Upper Andesite Member. The upper andesite member is exposed on the north flank of San Antonio Mountain. Individual flows are vesicular, dark grey, and aphanitic and can be traced for as much as 1.6 km (1 mi). In thin section, the rock is intersertal with some specimens showing pilotaxitic patches. Hypersthene phenocrysts are set in a groundmass of plagioclase, augite, hypersthene, opaque minerals and brown glass. Hypersthene phenocrysts are 0.5-1.5 mm and are subhedral and prismatic in shape. Euhedral to subhedral groundmass grains are <0.3 mm in size.

Basalt of Piñabetoso Peak

The basalt of Piñabetoso Peak consists of interlayered cinder and lava cones and associated flows erupted from a vent located east of San Antonio Mountain. The lava flows are vesicular black basalt, containing numerous quartz xenocrysts and feldspar megacrysts set in an aphanitic groundmass. Thin sections have plagioclase megacrysts and phenocrysts of augite, olivine, hypersthene and plagioclase in an intersertal groundmass of plagioclase, augite and opaque minerals. Plagioclase megacrysts are rounded and partially resorbed, and range from 0.2-2.0 mm. Hypersthene and plagioclase phenocrysts are 0.2-1.5 mm are are euhedral to anhedral. Olivine phenocrysts are euhedral to subhedral and are 0.1-0.4 mm. Augite phenocrysts are subhedral and 0.1-0.7 mm. Groundmass grains are <0.1 mm.

The basalt of Piñabetoso Peaks has been dated by the K-Ar method at 1.80 ± 0.72 m.y. (P.W. Lipman, personal communication, 1975).

Quaternary Units

Rock Glaciers

Rock glaciers are found in isolated localities on north and west flanks of San Antonio Mountain. They cover <0.64 km^2 (0.25 mi^2) and consist of angular to rounded gravel forming glacier-like masses up to 0.5 km long (Fig. 12).

Colluvium

Colluvium deposits are found on the lower flanks of San Antonio Mountain in the west, north and east. They consist of lobate, flow-like deposits which may have been deposited by solifluction. Individual lobes are formed by unconsolidated silt, sand and gravel. The total exposure is $<2.5\ km^2$ ($1\ mi^2$).

Alluvium

Alluvium was mapped over $38\ km^2$ ($15\ mi^2$) and consists of unconsolidated silt, sand and gravel. It was mapped where deposits were sufficiently thick to obscure contact relationships.

Figure 11. Rock glacier on the northern side of San Antonio mountain. Most blocks are ~0.5 m in size.

PETROLOGY

General Statement

Rock names assigned to units within the field area were based primarily on normative mineralogy, using Travis (1955) as a guideline. Secondary emphasis was placed on modal mineralogy. In general, rock names correspond to the following silica percentages:

Basalt	<52% SiO_2
Basaltic Andesite	52-56% SiO_2
Andesite	56-62% SiO_2
Latite	62-65% SiO_2

Whole-rock analyses for major-element oxides were determined by Marcia E. Register, University of New Mexico, using the following techniques: silica was determined gravimetrically; total Fe, Al_2O_3, MgO, CaO, Na_2O, K_2O, TiO_2, MnO and SrO were determined by atomic absorption (using calibration curves prepared from basalt standard UNM B-1 and standardized in turn against U.S.G.S. standard BCR-1); P_2O_5 was determinedcolorimetrically with ammonium molybdate, and FeO was determined by titration with $K_2Cr_2O_7$. Water was determined indirectly by loss on ignition, taking into account the amount of ferrous iron which was oxydized to ferric iron. Whole rock analyses and calculated norms are listed in Table 3.

Chemistry

Basalts and basaltic andesites, plotted on an Na_2O + K_2O vs. SiO_2 diagram (Fig. 12), fall within the tholeiite field of MacDonald and Katsura (1964), except for the alkali basalt member of the

Table 3. Wet chemical analyses for San Antonio Mountain field area rocks.

	1	2	3	4	5	6	7	8
SiO_2	53.67	50.02	50.78	49.96	52.52	55.88	56.40	58.27
Al_2O_3	15.67	16.40	16.99	15.85	14.10	14.95	15.15	15.40
FeO	7.44	7.30	5.43	8.63	7.80	3.59	6.47	3.68
Fe_2O_3	1.98	3.70	3.32	2.26	2.93	4.31	4.04	3.11
MgO	6.40	7.59	6.10	7.75	6.20	5.90	2.32	3.25
CaO	6.65	9.03	8.12	8.55	9.31	6.90	5.55	6.00
Na_2O	3.25	2.84	3.82	3.10	2.98	3.28	3.70	4.30
K_2O	1.45	0.37	2.29	0.62	0.87	1.50	2.32	2.74
TiO_2	1.05	1.10	1.52	1.31	1.40	0.94	1.81	1.03
MnO	0.15	0.16	0.14	0.16	0.16	0.14	0.14	0.10
Sro	0.03	0.02	0.07	0.04	0.04	0.03	0.05	0.09
H_2O+	0.20	0.20	0.06	0.14	0.20	0.18	0.06	0.14
H_2O-	1.11	0.87	0.40	0.06	1.91	1.28	1.37	0.89
P_2O_5	0.24	0.20	0.69	0.23	0.26	0.15	0.66	0.50
	99.29	99.80	99.73	99.66	100.68	99.75	100.04	99.50
Q	2.77	0.66	0.00	0.00	3.47	8.31	13.13	7.37
Or	8.75	2.22	13.55	3.72	5.27	9.09	14.22	16.45
Ab	29.75	25.88	34.55	28.25	27.41	30.22	34.46	39.24
An	24.31	31.38	22.49	27.92	23.09	22.21	18.55	14.87
Di	6.22	10.22	10.68	10.89	17.95	9.53	4.43	9.66
Hy	24.03	23.69	0.37	18.03	17.11	15.11	4.43	6.53
Wo	0.00	0.00	0.00	0.00	0.00	0.00	0.00	0.00
Ol	0.00	0.00	11.52	6.46	0.00	0.00	0.00	0.00
Ne	0.00	0.00	0.00	0.00	0.00	0.00	0.00	0.00
Mt	2.11	3.97	3.48	2.40	3.14	3.85	6.16	3.30
Il	1.49	1.56	2.12	1.85	2.00	1.34	2.62	1.46
Ap	0.51	0.42	1.44	0.49	0.58	0.32	1.43	1.06
	99.94	100.00	100.20	100.01	100.02	99.98	99.43	99.99

1- Wissmath Craters Basalt xenocrystic tholeiite member
2- Wissmath Craters Basalt olivine tholeiite member
3- Wissmath Craters Basalt alkali basalt member
4- Servilleta Basalt
5- Malette Creek basaltic andesite
6- Red Hill basaltic andesite
7- Los Cerritos de la Cruz basaltic andesite
8- San Antonio Mountain volcanic complex first lower andesite member

Table 3 continued. Wet chemical analyses for San Antonio Mountain field area rocks.

	9	10	11	12	13	14	15	16
SiO_2	59.94	64.74	55.41	60.38	51.51	57.37	62.06	73.72
Al_2O_3	15.00	14.75	16.40	15.30	16.48	16.20	15.90	13.10
FeO	3.02	3.31	6.27	2.97	6.27	3.61	2.21	
Fe_2O_3	3.09	1.62	3.78	2.20	3.78	3.49	3.29	0.71
MgO	2.90	2.15	6.45	2.72	6.45	4.75	2.47	0.01
CaO	6.15	3.85	7.85	5.40	7.85	5.70	4.48	0.89
Na_2O	3.78	3.98	3.20	3.98	3.20	4.07	3.78	3.88
K_2O	3.17	3.30	1.09	3.25	1.09	1.98	3.13	4.53
TiO_2	0.78	0.62	1.29	0.75	1.29	0.90	0.70	0.08
MnO	0.09	0.07	0.16	0.12	0.16	0.12	0.09	0.07
SrO	0.07	0.05	0.03	0.08	0.03	0.07	0.07	
H_2O+	0.16	0.06	0.02	0.08	0.02	0.34	0.10	
H_2O-	1.54	0.21	0.39	1.44	0.39	0.22	0.46	
P_2O_5	0.60	0.31	0.25	0.47	0.25	0.39	0.45	
	100.29	99.02	99.23	99.13	99.23	99.23	99.18	96.99
Q	11.08	16.57	5.13	10.76	2.08	7.50	15.46	
Or	19.09	19.83	16.05	19.68	6.57	11.82	18 85	
Ab	34.59	36.35	41.41	36.64	29.30	36.94	34.60	
An	14.88	12.86	13.62	14.65	27.71	20.31	17.51	
Di	9.78	3.61	8.79	7.74	8.28	4.56	1.73	
Hy	4.90	7.53	6.30	6.10	19.66	13.09	6.39	
Wo	0.00	0.00	0.00	0.00	0.00	0.00	0.00	
Ol	0.00	0.00	0.00	0.00	0.00	0.00	0.00	
Ne	0.00	0.00	0.00	0.00	0.00	0.00	0.00	
Mt	3.29	1.72	4.39	2.36	4.03	3.69	3.51	
Il	1.11	0.88	2.21	1.07	1.83	1.27	0.99	
Ap	1.28	0.66	2.10	1.01	0.53	0.82	0.96	
	100.00	100.04	100.00	100.01	99.99	100.00	100.00	

9- San Antonio Mountain second lower andesite member
10- San Antonio Mountain latite member
11- San Antonio Mountain upper basaltic andesite member
12- San Antonio Mountain upper andesite member
13- Pinabetoso Peaks basalt
14- Cerro de la Olla
15- Ute Mountain
16- No Agua Mountain (Naert, 1974)

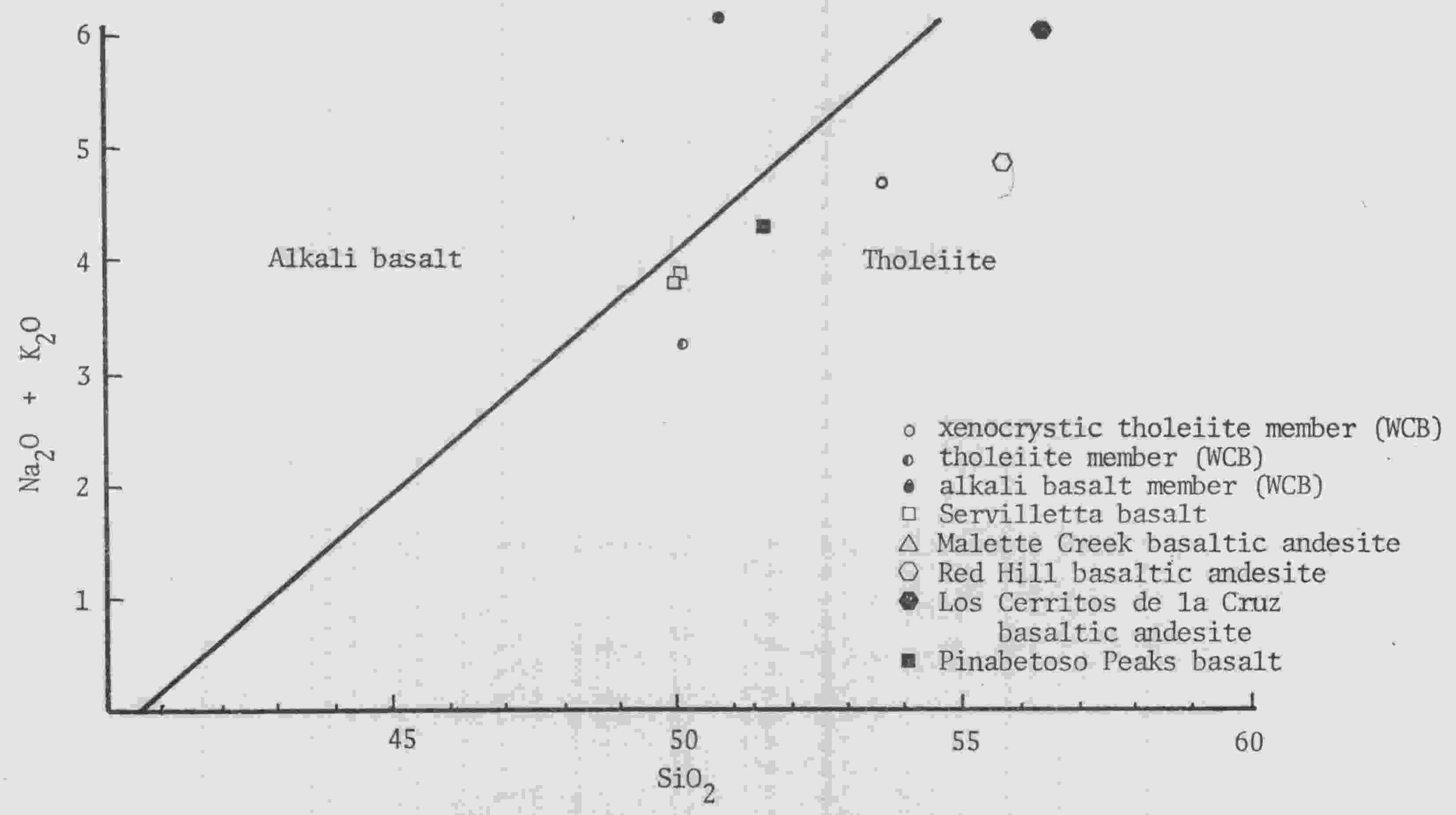

Figure 12. Plot of total alkalis vs silica for the San Antonio Mountain field area basaltic rocks. Boundary line from MacDonald and Katsura (1964).

Wissmath Craters basalt. Norms also confirm the tholeiitic affinities, as most of the units are hypersthene-normative. Again, the alkali basalt member is the exception, with 11.5 percent normative olivine and only 0.37 percent normative hypersthene. The origin of an alkali basalt within an almost exclusively tholeiitic terrane is uncertain.

The alkali-lime index of 59 (Fig. 13) indicates that rocks from the San Antonio Mountain area are calc-alkalic. The AMF plot (Fig. 14), shows earlier basalts to fall on the calc-alkalic differentiation trend whereas later rocks plot above the trend.

Harker diagrams (Fig. 15 and 16) and the AMF plot (Fig. 14) appear to indicate three separate variation trends. The first involved basaltic rocks which erupted early. A Harker plot of these rocks (Fig. 15) indicate that later flows generally became enriched in K_2O and Na_2O and depleted in FeO, CaO, MgO and Al_2O_3. The second trend involves the early andesites and latite of the San Antonio Mountain volcanic complex (sequence 1-2, Fig. 16; 3-4, Fig. 14). The rocks appear to follow calc-alkalic trends, with the latite enriched in alkalies and depleted in MgO, CaO and total Fe relative to the earlier andesites. The third trend, indicated by the late basaltic andesite and andesite of San Antonio Mountain, appears to follow calc-alkalic trends on the Harker diagram (Fig. 16, sequence 3-4), but the AMF plot appears to suggest Fe enrichment (Fig. 14, sequence 5-6) for the late andesite rather than alkali enrichment.

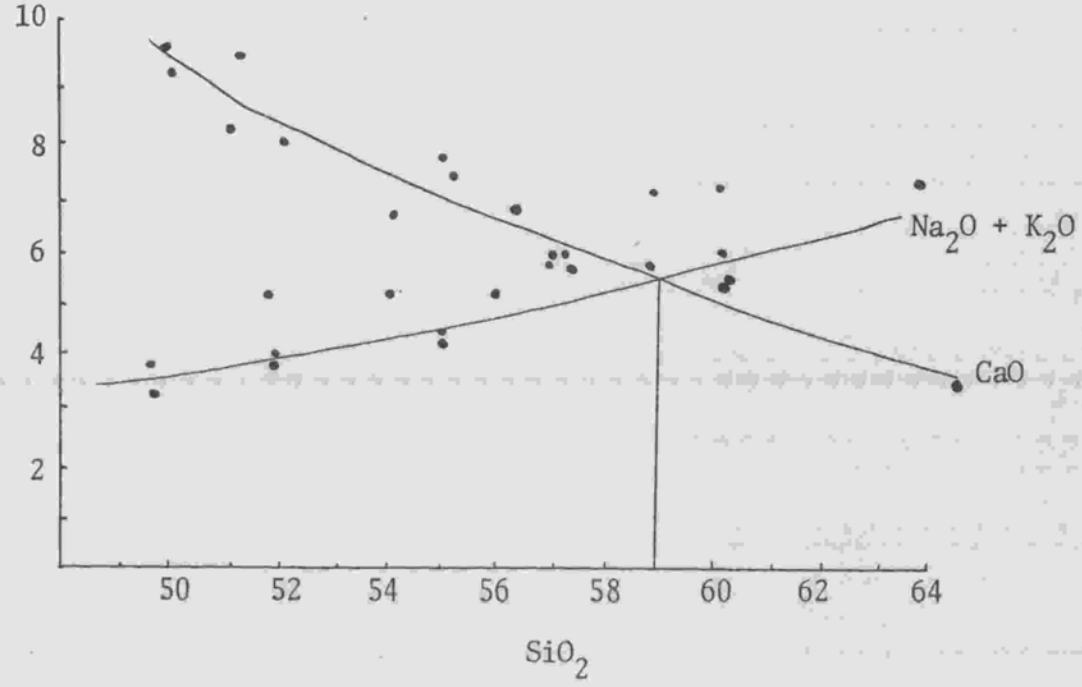

Figure 13. Alkali-lime index determination for the San Antonio Mountain area rocks.

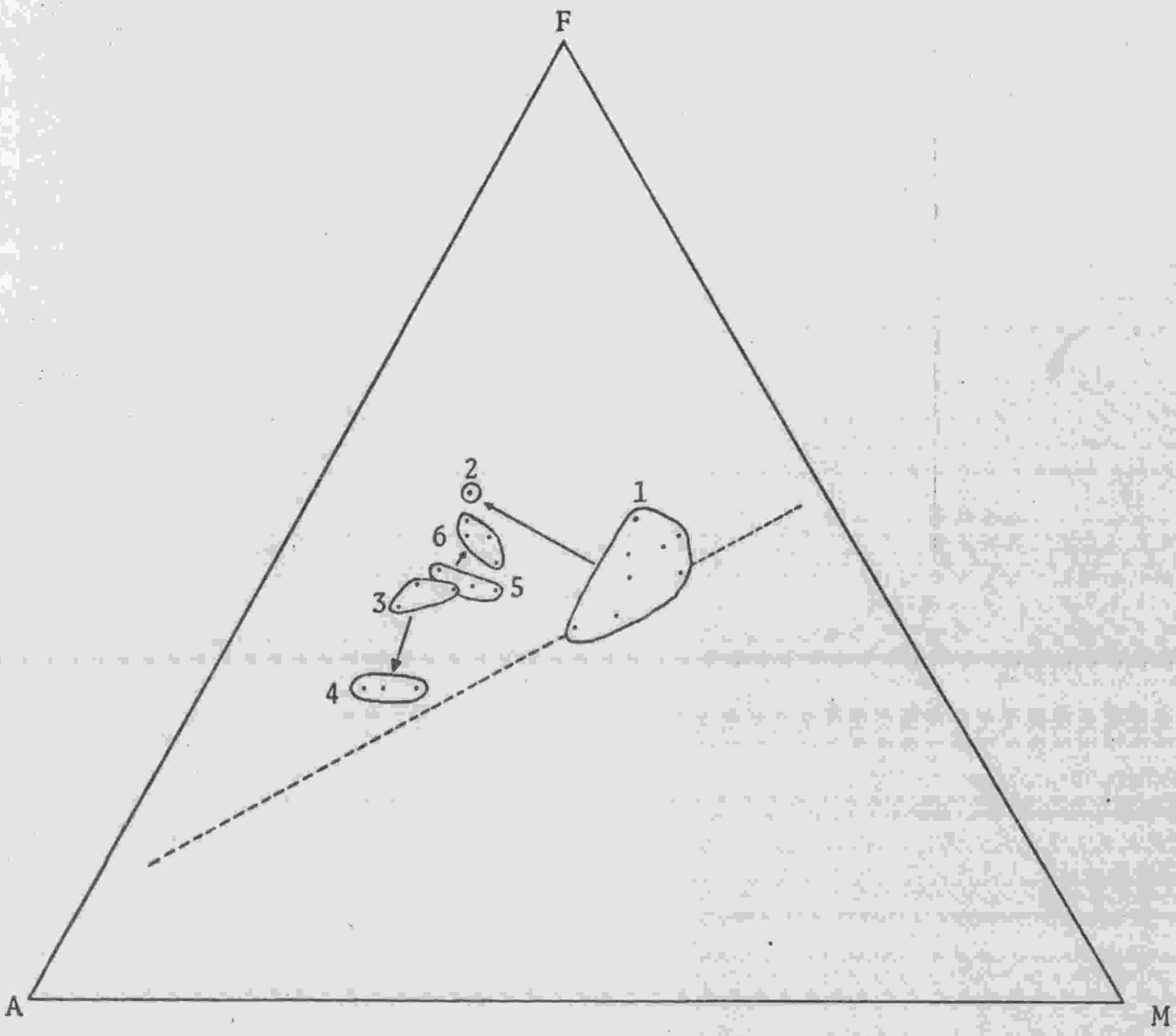

Figure 14. AMF plot of the San Antonio Mountain area rocks. Dashed line indicates calc-alkaline differentiation trend. Numbered fields indicate possible variation groups for the field area rocks.

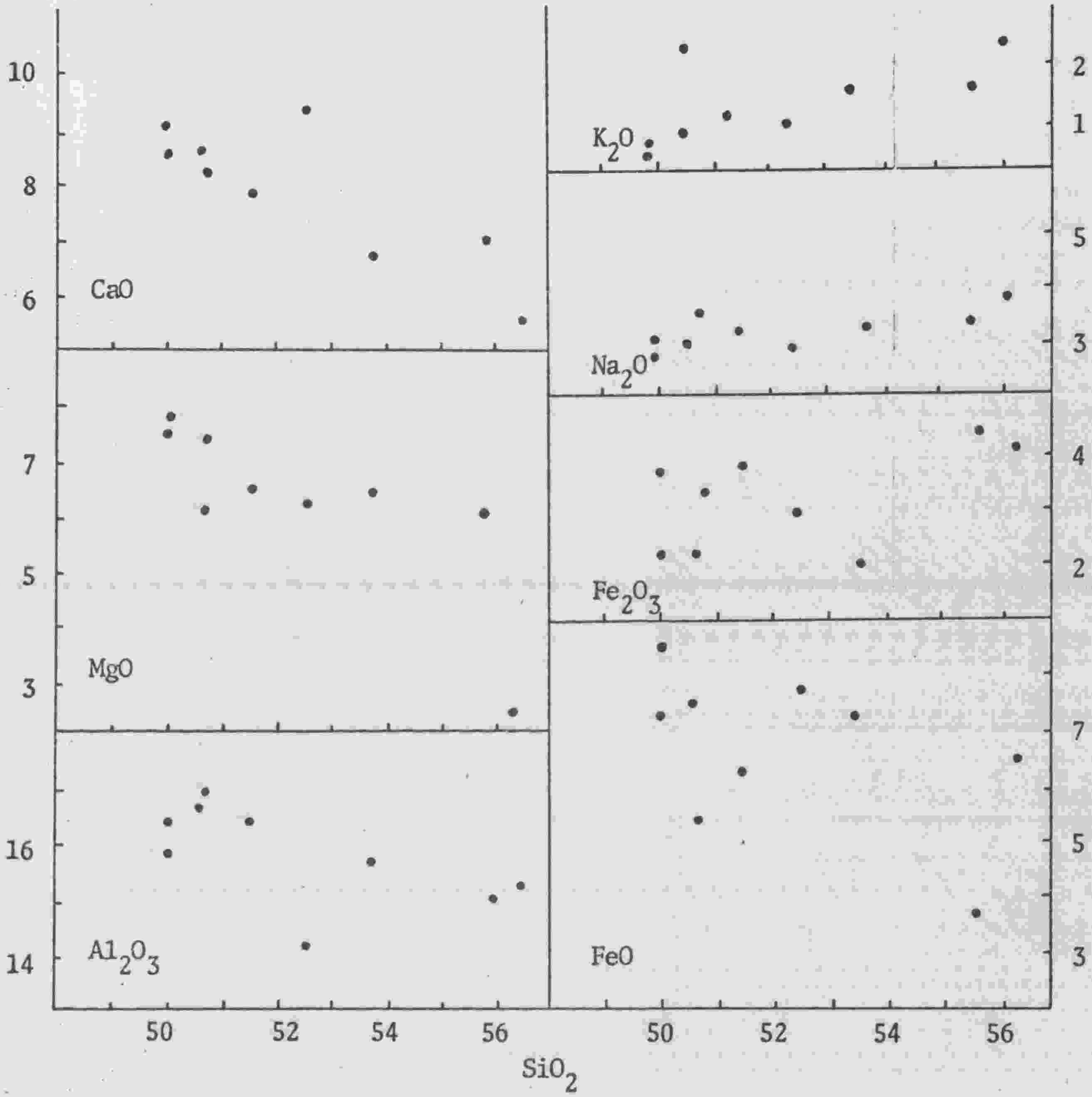

Figure 15. Harker variation diagrams for the basaltic rocks of the San Antonio Mountain area.

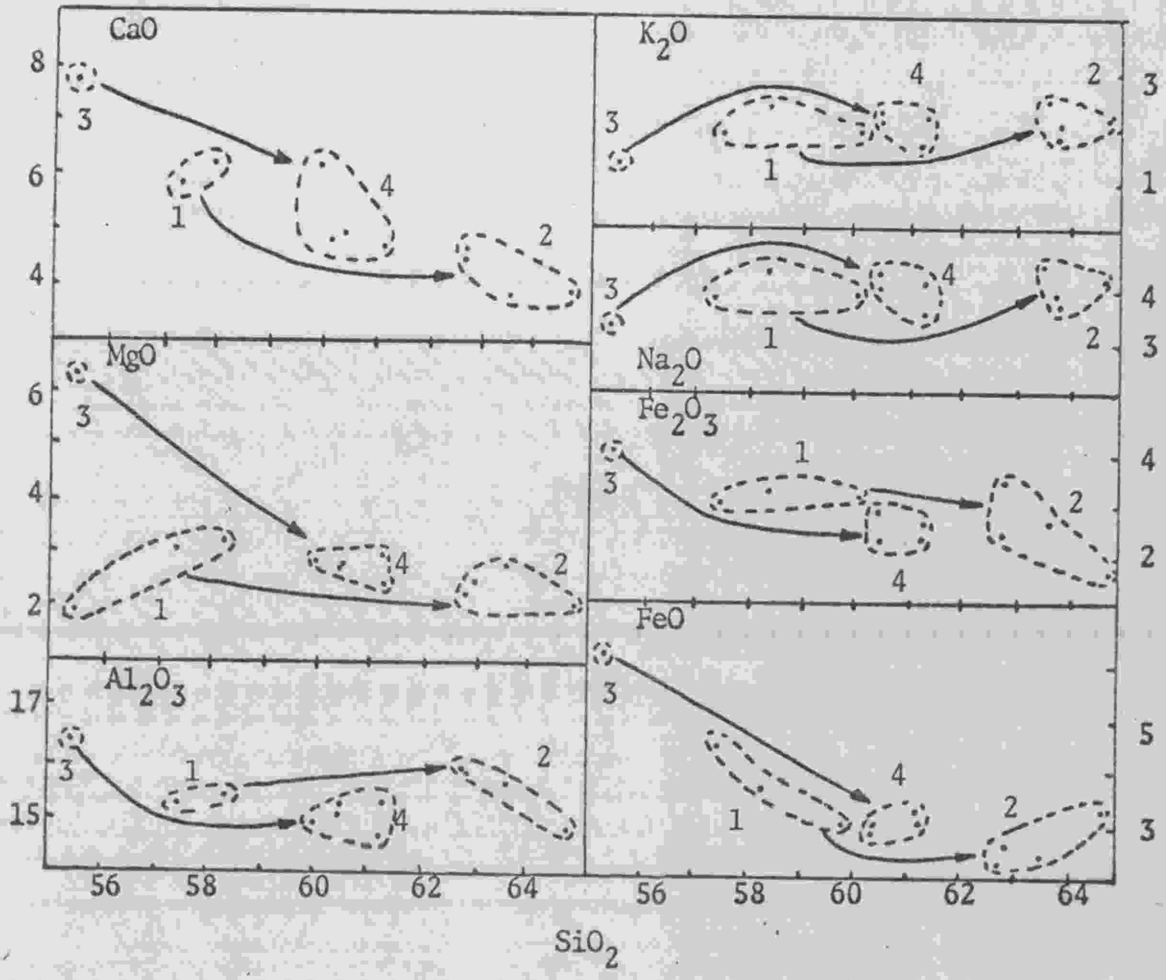

Figure 16. Harker variation diagrams for the San Antonio Mountain volcanic complex. 1-lower andesite, 2-latite, 3-late basaltic andesite, 4-late andesite.

Individual latite flows appear to have a slight chemical zonation related to the four subunits (Table 4). Silica percentage appears to decrease toward the outer edge of the flows. The reason for this is not known.

Comparison of San Antonio Mountain Area Volcanics With Other Volcanic Centers of the Region

Three volcanic centers within the San Luis Basin were chosen to provide a chemical comparison with the San Antonio Mountain area volcanics. Ute Mountain is located on the eastern side of the San Luis Basin near the Colorado-New Mexico border and is a latitic volcano similar to San Antonio Mountain. Cerro de la Olla is an olivine andesite volcano located 32 km (20 mi) east-southeast of San Antonio Mountain. Both Cerro de la Olla and Ute Mountain were sampled on reconnaissance tranverses. No Agua Mountain is a cluster of rhyolite domes located 8 km (5 mi) south of Wissmath Craters. The mountain was mapped extensively by Naert (1974) and chemical analyses were obtained from his work. Chemical analyses for lavas from all three volcanos are given in Table 3. Cerro de la Olla appears to be intermediate in composition between the basaltic and latitic rocks of the San Antonio Mountain area. The Ute Mountain rocks are compositionally similar to San Antonio Mountain latite while the No Agua rhyolites are richer in alkalies than any of the rocks of the San Antonio Mountain area.

Table 4. Chemical variations between latite sub-units. 1 - black glassy sub-unit, 2 - silver platy sub-unit, 3 - silver holocrystalline sub-unit, 4 - black scoriaceous sub-unit.

	1	2	3	4
SiO_2	64.7	63.5	62.3	62.8
Al_2O_3	14.8	15.7	16.5	15.8
FeO	1.6	2.4	2.2	2.6
Fe_2O_3	1.6	2.5	2.9	2.3
MgO	2.2	1.9	2.0	2.3
CaO	3.9	3.9	4.3	4.8
Na_2O	4.0	4.3	3.9	3.6
K_2O	3.3	3.3	3.0	3.5
TiO_2	0.6	0.7	0.6	0.7
MnO	0.07	0.07	0.08	0.09
SrO	0.06	0.06	0.06	0.06
H_2O^+	0.21	0.581	0.46	1.394
H_2O^-	0.06	-0.019	0.10	0.12
P_2O_5	0.2	0.34	0.4	0.3
Total	99.0	99.2	99.3	100.0

Petrogenesis

Any hypothesis for the composition and number of parent magmas for the volcanic rocks of the San Antonio Mountain field must take into account the following evidence. (1) The units have calc-alkalic affinities; (2) AMF and Harker diagrams indicate that there are three distinct variation trends involving the early basaltic rocks, the early andesites and latite of San Antonio Mountain, and the late basaltic andesite and andesite of San Antonio Mountain; (3) the most widespread unit, the Servilletta basalt, occurs throughout the San Luis Valley, in contrast to the limited areal extent of the other volcanic units. In addition, the Servilletta basalt has a distinctive coarse-grained, diktytaxitic texture which contrasts sharply with the other rocks of the area; (4) the youngest volcanic unit in the field area, the basalt of Piñabetoso Peaks, has approximately the same composition as the oldest basalt unit, the basalt of Wissmath Craters.

On the basis of this evidence, it is possible to postulate that two parent magmas were responsible for the rocks of the field area. One, which was olivene tholeiite in composition was the parent of the basalts of the Servilletta Formation; the second, which may have been basaltic in composition was parental to the calc-alkalic suite comprised of the early basaltic rocks and the San Antonio Mountain volcanic complex.

The second magma is postulated on the basis of the observed calc-alkalic affinities on Harker and AMF diagrams. In addition, the petrographic and mineralogic similarities of many of the units argues for their derivation from the same source.

The three separate trends seen on the Harker plots and the AMF diagram may indicate that three separate bodies of magma were emplaced beneath the field area at different times and in different locations. All three magmas originated from calc-alkalic source magma and were emplaced and evolved independently of each other to produce the following sequences of rocks (Fig. 17): (1) the early basaltic magma erupted the Wissmath Craters Basalt initially and subsequently erupted more MgO-poor basaltic andesites culminating with the Los Cerritos de la Cruz basaltic andesite; (2) San Antonio Mountain magma "A" erupted the two lower andesites and the latite, becoming progressively enriched in SiO_2 and alkalis with decreasing age; (3) San Antonio Mountain magma "B" erupted the upper basaltic andesite and andesite units, becoming increasingly Fe-rich with time. The chemical evolution of each magma may be the result of fractionation, crustal contamination, or both. The Piñabetoso Peaks basalt may have been derived directly from the calc-alkalic source magma and erupted with no significant chemical evolution. Alternatively, this basalt may have been derived from an entirely different source.

The manner in which the separate bodies of magma were segregated is not known. Higgins (1973), in explaining petrologic differences seen at Newberry Caldera, Oregon, speculated that "magma conduits

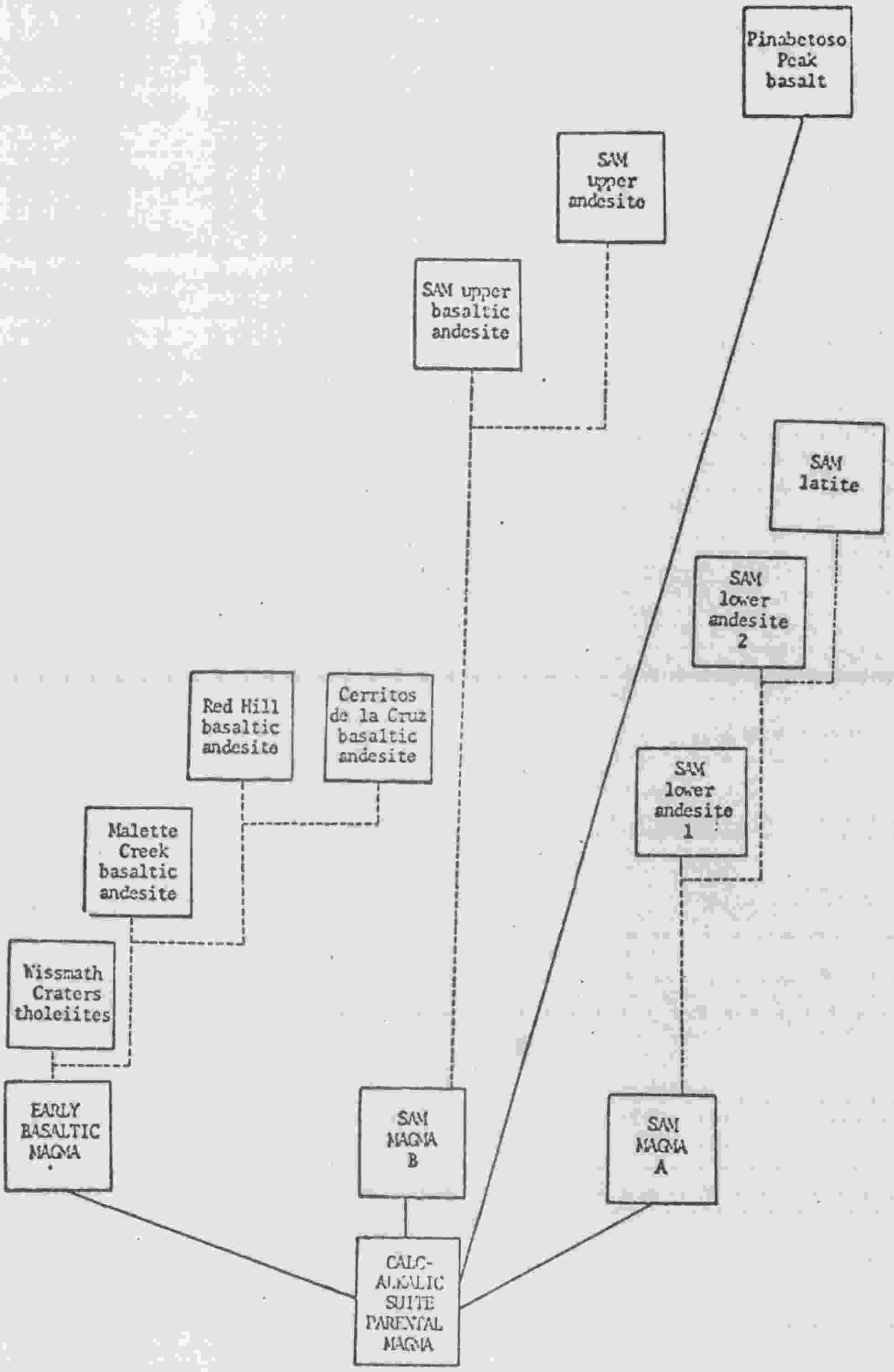

Figure 17. Schematic diagram of the possible evolution of the magma which produced the San Antonio Mountain area rocks. Dashed lines indicate crustal contamination or differentiation; solid lines indicate emplacement into higher crustal levels.

were probably a gridlike plexus of intersecting dikes and fissures, with . . . magma pockets at grid intersections. Magma was trapped in shallow chambers and periodically released by faulting. The entrapment of magma allowed differentiation in smaller chambers". A similar situation may have existed beneath the San Antonio Mountain area.

MORPHOLOGY AND STRUCTURE

General Statement

The volcanos of the San Antonio Mountain area can be classified into four groups: cones built from interlayered cinder and lava (north and south Piñabetoso Peaks), lava cones (north and south Los Cerritos de la Cruz), tholeiite shield volcanos (Wissmath Craters), and flow domes (San Antonio Mountain).

The morphology of individual volcanos was characterized using qualitative descriptions and aspect ratios (height/width) and maximum slope angles (Table 5). The internal structures were inferred on the basis of field observations. Assymetry of individual volcanos was classified as follows: (1) primary assymetry, caused by conditions at the vent during eruption, (2) secondary assymetry, caused by late stage activity, such as explosion or collapse, and (3) assymetry caused by post-formation erosion.

Cinder and Lava Cones

The north and south Piñabetoso Peaks form two cinder cones which have interlayered lava which intrudes the pyroclastic material. A set of profiles of each cone is shown in Figure 18.

The two cones are almost identical in size. The north cone is 372 m (1200 ft) wide and 24 m (78 ft) high and the southern cone is 434 m (1400 ft) wide and 22 m (71 ft) high. Both cones are composed of cinders and spatter which have been intruded by

Table 5. Aspect ratios and maximum slope angles for the volcanos of the field area and regional volcanic centers.

	Aspect Ratio	Maximum slope angle
Wissmath Craters	0.019	2°
Pinabetoso Peaks		
North	0.065	too eroded to measure accurately
South	0.051	
Los Cerritos de la Cruz		
North	0.096	34°
South	0.150	26°
Red Hill	0.092	21°
San Antonio Mountain	0.099	16°
Ute Peak	0.104	19°
Cerro de la Olla	0.063	11°
No Agua Mountain	0.147	23°

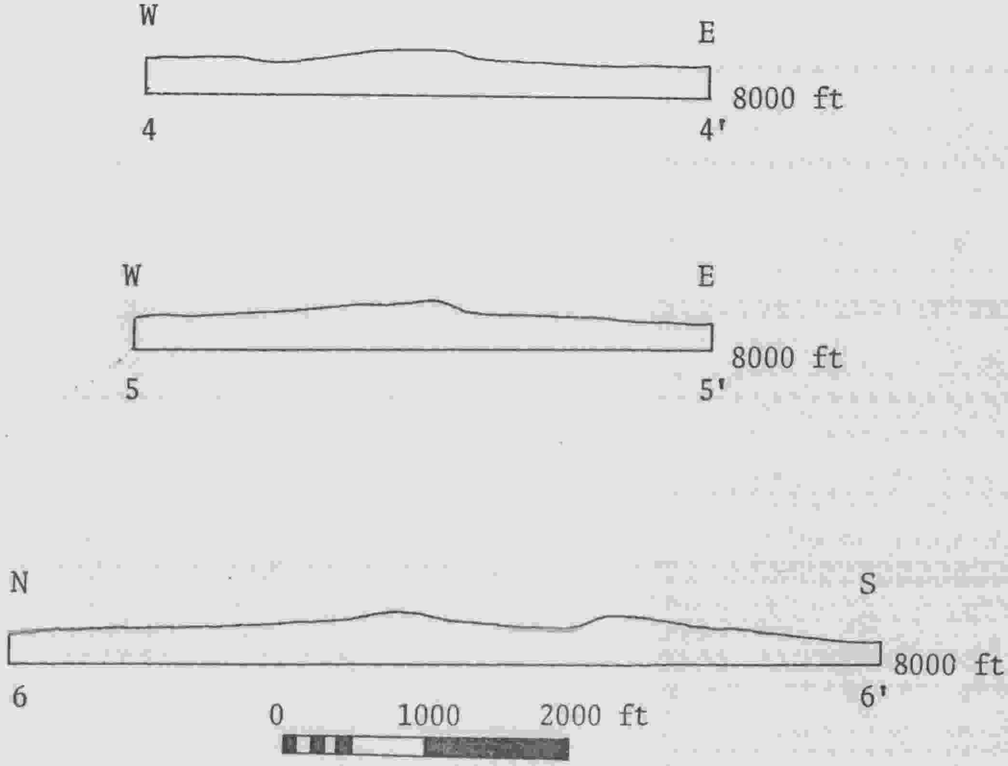

Figure 18. Profiles of the Piñabetoso Peaks. Location of profile lines given on Figure 1c. No vertical exaggeration.

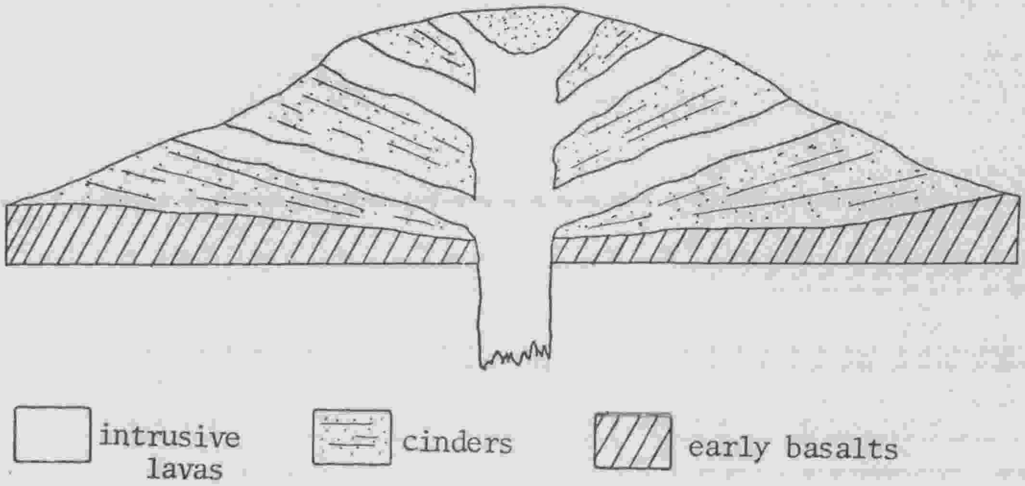

Figure 19. Schematic cross section of the northern Piñabetoso Peak showing the relationship between early extrusive basalts, cinders and intrusive lavas.

lava. The north cone is symmetrical. The south cone, however, is asymmetrical, with a steep east side and a gently sloping west side. The asymmetry appears to be primarily erosional; the intruding lavas appear to have buttressed the cones, making them more resistant to erosion. The southern cone was intruded only on its eastern flank; consequently its western flank was more susceptible to erosion and formed the gradual slope seen today. Because of the degree of erosion, it is impossible to determine if there was any primary or secondary asymmetry in the Piñabetoso Peaks.

The internal structure of the cones can be inferred from field relations. The intruded lavas dip inward (Fig. 19) with dip angles of 25°-75°, and are grouped around the center of the cone in an elliptical shape. The long axis of the ellipse is oriented north. The dip angles of the intrusions become steeper at higher stratigraphic levels in the cone. It appears that the lavas have emanated from a common feeder (Fig. 19) after the pyroclastic materials were deposited.

Lava Cones

The north and south Cerritos de la Cruz and Red Hill form lava cones in the southern portion of the field area. Profiles of each are given in Figures 20 and 21).

Los Cerritos de la Cruz

The north and south Cerritos de la Cruz have different shapes, probably because of their differing eruptive histories.

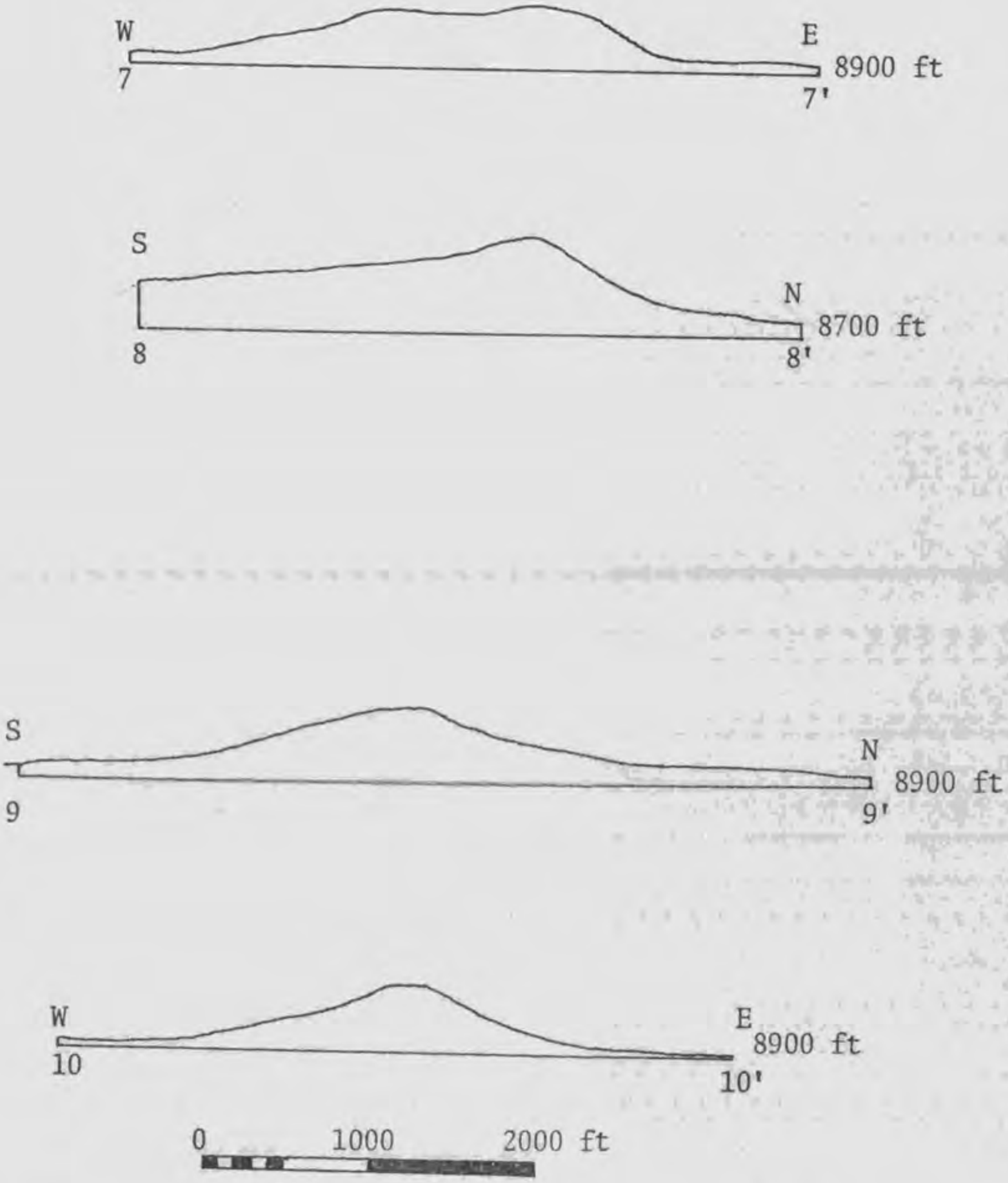

Figure 20. Profiles of the north and south Cerritos de la Cruz.

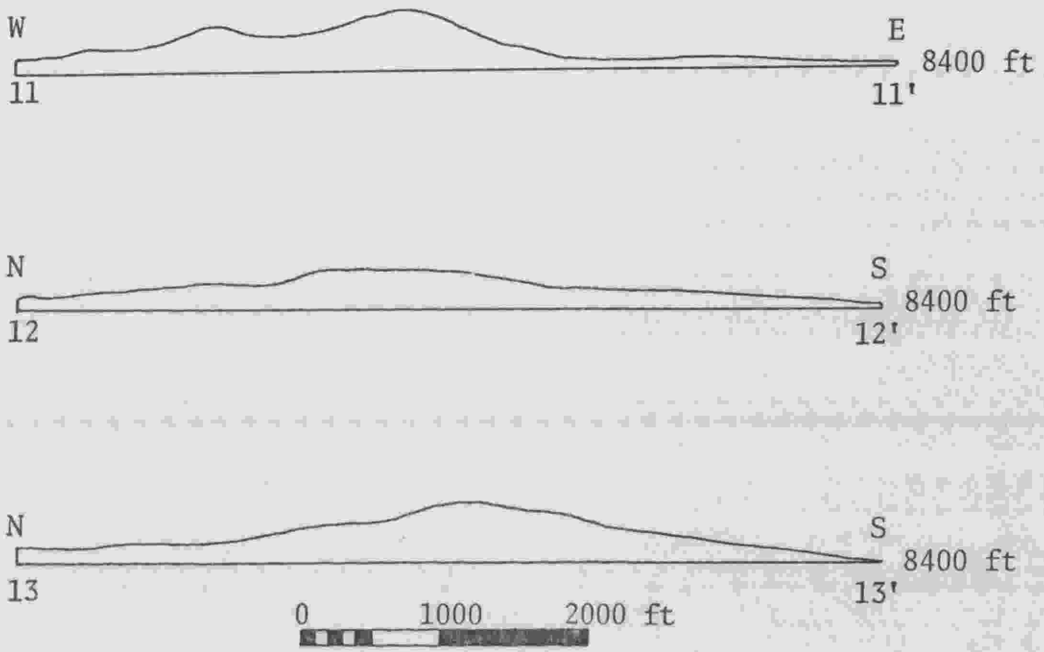

Figure 21. Profiles of Red Hill.

The northern cone is 630 m (2100 ft) wide and 71 m (237 ft) high and the southern cone is 1230 m (4100 ft) wide and 123 m (410 ft) high. The southern cone is symmetrical while the northern cone is completely breached on its south end. The secondary asymmetry caused by the breaching is probably related to late stage explosive activity, similar to that proposed by Kelley (1974) for several cones in the Albuquerque volcanic field. There does not appear to be any extensive erosion of either volcano.

The internal structure of the northern cone is complex. On the outer flanks of the volcano, flow units dip outward with dip angles not exceeding the maximum slope angle. In the interior of the cone, flow units dip inward around the breached section, forming an amphitheater.

The internal structure of the southern cone is not known, because of lack of dissection. On the flanks, the flow units dip away from the center of the cone. The interior of the structure of the volcano may be a succession of outward dipping flow units which were erupted from a progressively higher vent.

Red Hill

Red Hill is a breached lava cone similar to the northern Cerrito de la Cruz. The volcano is 1050 m (3500 ft) wide and 94 m (312 ft) high. Red Hill is asymmetrical, with its east flank 50 m higher than its west flank (Fig. 21). The asymmetry is primary. Porter (1972) reported similar asymmetry in cinder and scoria cones in Hawaii and attributed it to either vent conditons or changing wind direction. Since the cone is mostly composed of lava flows, wind direction did not have an appreciable effect on the primary asymmetry of Red Hill. The cone is breached at its southern end, probably by an explosion. There does not appear to be appreciable erosion of Red Hill. The internal structure of Red Hill is not known as the explosion appears to have disrupted the original structure of the cone.

Tholeiite Shield Volcanos

The Wissmath Craters tholeiite shield has a height of 62 m (200 ft) and a width of 5766 m (18,600 ft). These dimensions are based on the extent of the latest unit extruded from the vent, which is responsible for the present morphology of the volcano (Fig. 22). However, the structure has been covered by Servilletta Basalt in the north, and its complete shape is unknown.

The summit of the volcano has an irregular crater which is 2,000 m (6,600 ft) long, 400 m (1,320 ft) wide, and 31 m (100 ft) deep (Fig. 23). The exposure of a section of Wissmath Craters basalt in the crater walls suggest that the crater formed by collapse of the top of the volcano due to withdrawal of support from below. This occured late in the history of the shield, and probably was the result of draining of the magma chamber. The irregular form of the crater indicates that it may have originally been a series of overlapping craters.

The volcano has a primary asymmetry which is seen in the oldest basalt member extruded from the vent (Fig. 1). The

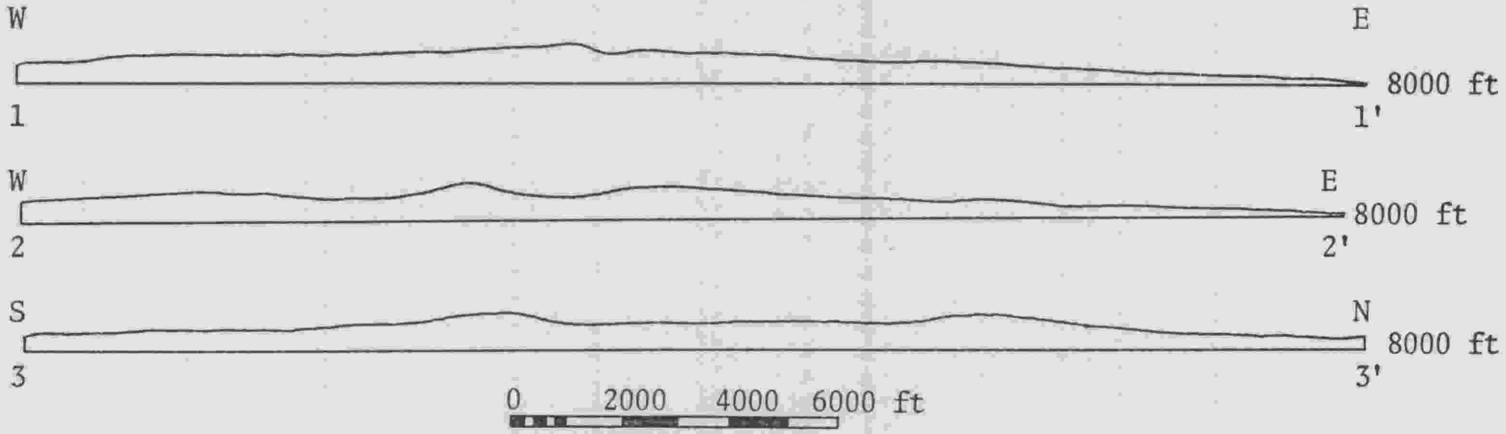

Figure 22. Profile of Wissmath Craters.

lavas appear to have flowed more extensively to the east. Erosional modification of the shield does not appear to be extensive.

The interior of the volcano probably consists of quaquaversally dipping lava flows which have very low dip angles. The central crater may have formed along a series of arcuate fractures; displacement along the fractures probably does not exceed 31 m (100 ft).

Flow Domes

San Antonio Mountain is described as a latite flow dome because it is a domical structure formed by successive eruptions of latite flows. The mountain is 660 m (2,200 ft) high and 9,000 m (30,000 ft) wide. Primary asymmetry appears to have been controlled by the eruptive history of the volcano. In Figure 24, east-west profile 16-16' has the most symmetric shape. It is probable that this shape is controlled by the eruption of one group of flows from a central vent, which covered the hill evenly, This portion of the hill is also seen in segment 2 of 17-17'. The less symmetric areas of the volcano may have been formed by later eruptions, either from a central vent, as in segment 3 of 17-17' and in profile 14-14', or by flank eruptions, as may be indicated in segment 1 of 17-17'. The major erosional modification of San Antonio Mountain is the large, central east-west valley (Fig. 24, 15-15'). The valley appears to have developed between young flows erupted on the southern half

Figure 23. Interior of Wissmath Craters. Note the abrupt break in slope on the right wall indicating the edge of the crater. The basin in the foreground is 300 m wide.

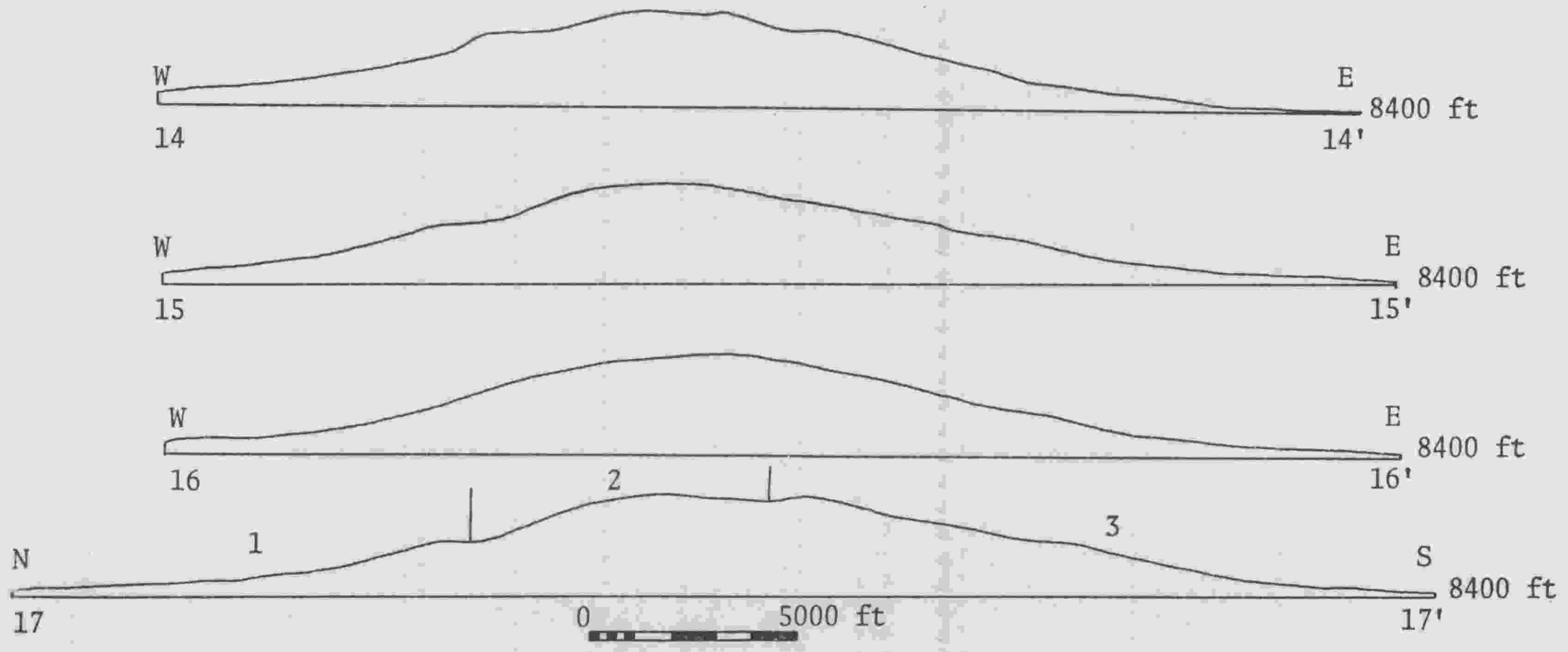

Figure 24. Profiles of San Antonio Mountain.

of the mountain and older flows erupted on the northern half. Other erosional activity may include some Pleistocene periglacinal activity. On the northern and western sides of the mountain, rock glaciers appear to have formed in some inter flow valleys, similar to those described by Chamberlin and Salisbury (1905, in Howe, 1909) in the San Juan Mountains of Colorado. However, there does not appear to be any evidence of Pleistocene glaciation.

The internal structure of San Antonio Mountain probably consist of quaquaversally dipping lava flows which have been erupted from at least 1 central vent. The dip angles on these flows does not exceed the maximum slope angle of 16°. A schematic cross section of the mountain is seen in Figure 1.

Correlation of Chemistry to External Morphology

Diagrams plotting silica percentage against aspect ratio and maximum slope angle are given in Figures 25 and 26). It appears that in larger structures, such as flow domes and shield volcanos, silica percentage is more important in determining external morphology than eruptive history or vent conditions. However, in the smaller volcanos, the opposite appears to be true.

A number of studies on basaltic volcanos have shown how eruptive history affects their shape. Heiken (1971) described volcanos from the Fort Rock-Christmas Lake valley basin, Oregon,

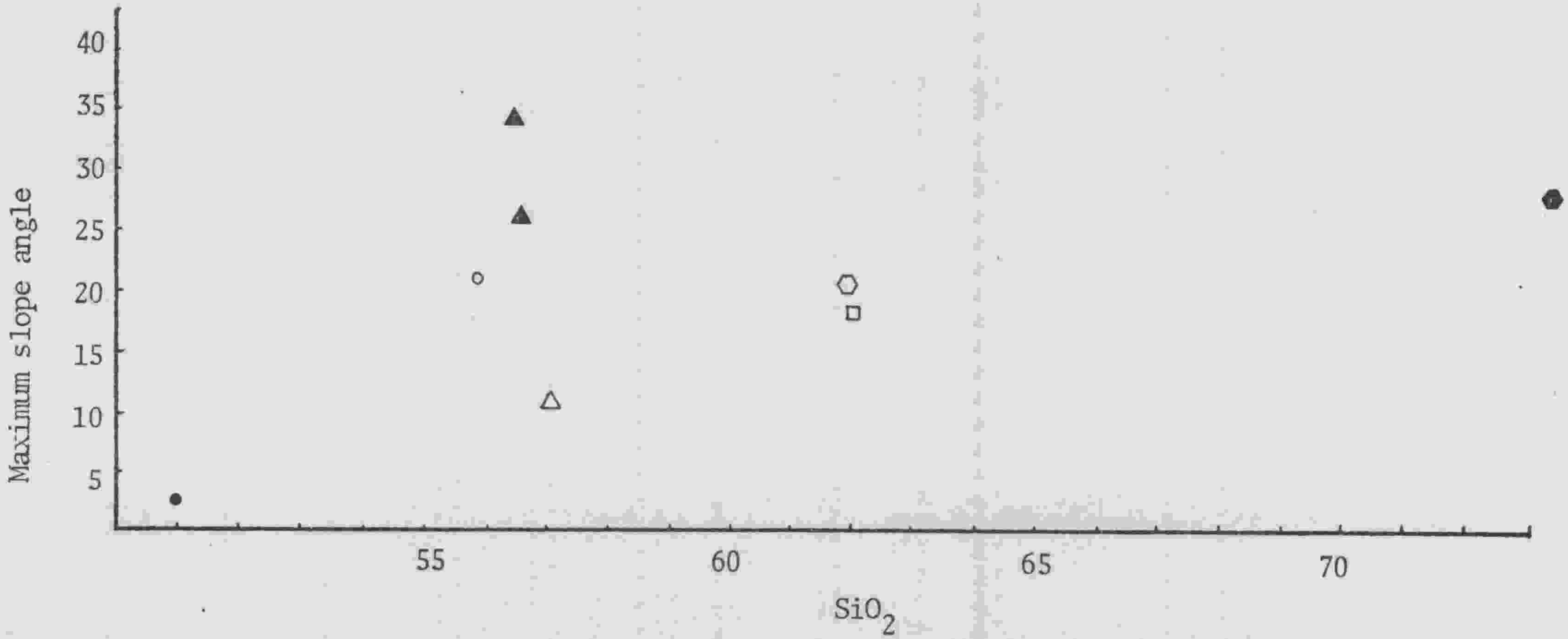

Figure 25. Plot of maximum slope angle vs SiO_2. Filled circle = Wissmath Craters, open circle = Red Hill, filled triangles = Los Cerritos de la Cruz, open triangle = Cerro de la Olla, open hex = Ute Mt., open square = San Antonio Mt., filled hex = No Agua Mt.

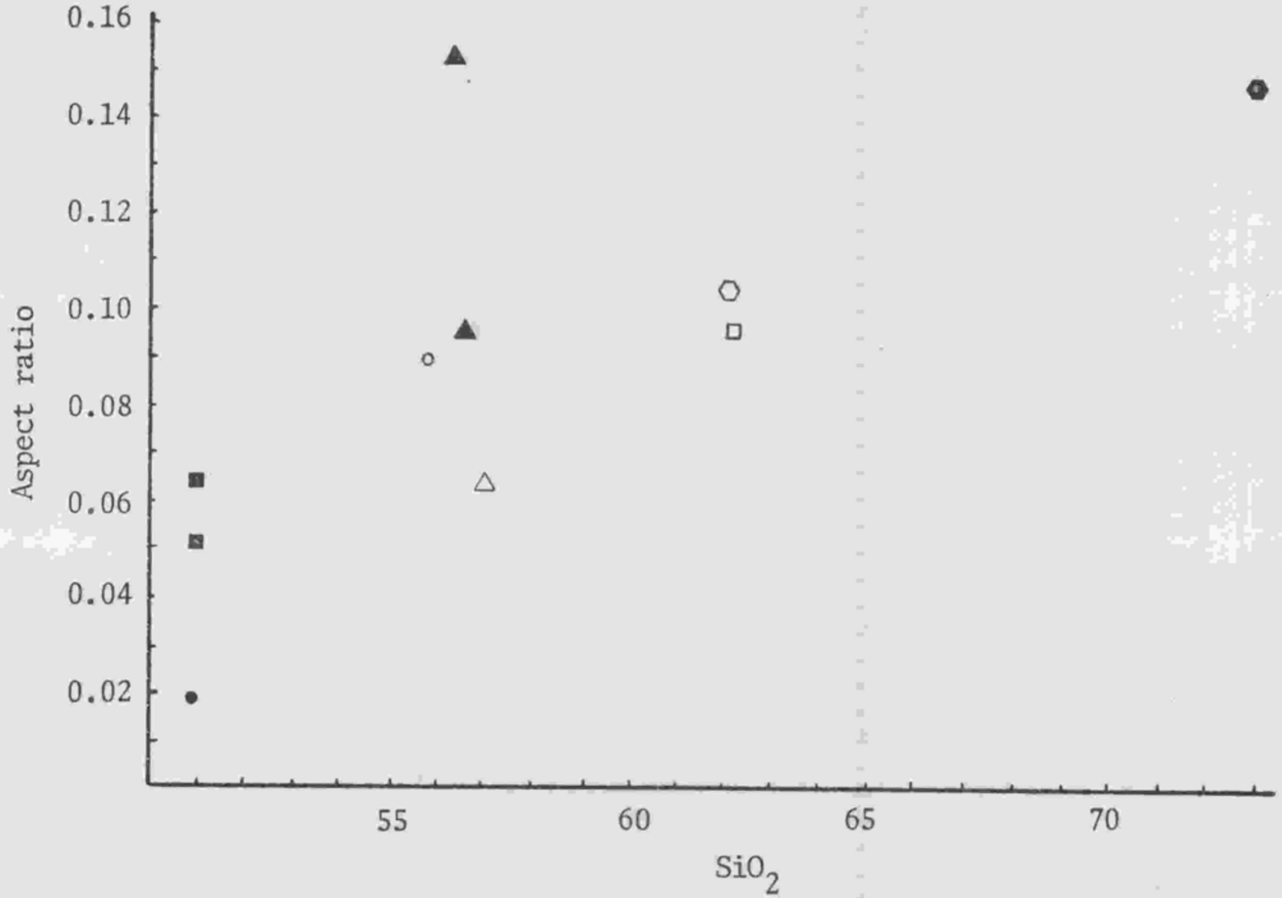

Figure 26. Plot of aspect ratio vs SiO_2. Symbol code same as in Figure 26, except for filled square = Piñabetoso Peaks.

which range from tuff rings (aspect ratios: 0.033-0.10) to cinder cones (aspect ratios: ~0.2). The variation is partly controlled by the depth at which the rising magma comes in contact with ground or surface water. When the depth of contact is great, eruptions occur through a vertical column and pyroclastics pile up close to the vent. Where the depth of contact is shallow, the eruption will cause a wider spread of pyroclastics and form tuff rings with low aspect ratios. Francis and Thorpe (1974) and Walker and Croasdale (1972) have reached similar conclusions. McGetchin _et al_. (1974), McGetchin and Head (1972) and Porter (1972) have found that the shape of cinder cones is a function of local wind conditions, velocity vector of the exiting pyroclastics and the gravity field strength.

Application of these studies to the volcanos of the San Antonio Mountain area indicate that shape is the result of both eruptive history and chemical composition. In flow domes (San Antonio Mountain, Ute Mountain, Cerro de la Olla) chemical composition will have a greater than eruptive history. The more siliceous the bulk composition, the more viscous the lava will be at a given temperature (Fig. 27 and 28) (Table 6). Consequently, flows will be thicker and will probably not travel as far from the vent as more fluid flows. This will result in larger maximum slope angles and larger aspect ratios. Deviations from this will result from later pyroclastic activity or parasitic flank eruptions. Flank

Table 6. Calculated theoretical viscosities for San Antonio Mountain field area samples and samples from regional volcanic centers. Viscosities equations and calculated viscosities derived using the method of Shaw (1972).

	viscosity, poises @ 1000°C	viscosity equation
Wissmath Craters Basalt		
xenocrystic tholeiite	5.171×10^4	$\ln V = 2.35*10^4/T-1.5*2.35-6.4$
olivine tholeiite	1.849×10^3	$\ln V = 2.19*10^4/T-1.5*2.19-6.4$
alkali basalt	4.939×10^3	$\ln V = 2.35*10^4/T-1.5*2.35-6.4$
Servilletta Basalt	2.171×10^3	$\ln V = 2.22*10^4/T-1.5*2.22-6.4$
Malette Creek basaltic andesite	2.670×10^3	$\ln V = 2.25*10^4/T-1.5*2.25-6.4$
Red Hill basaltic andesite	2.236×10^3	$\ln V = 2.44*10^4/T-1.5*2.44-6.4$
Los Cerritos de la Cruz basaltic andesite	1.715×10^4	$\ln V = 2.54*10^4/T-1.5*2.54-6.4$
San Antonio Mountain volcanic complex		
first lower andesite member	4.514×10^4	$\ln V = 2.69*10^4/T-1.5*2.69-6.4$
second lower andesite member	3.513×10^4	$\ln V = 2.65*10^4/T-1.5*2.65-6.4$
latite flow member	1.347×10^6	$\ln V = 3.23*10^4/T-1.5*3.23-6.4$
upper basaltic andesite member	1.723×10^4	$\ln V = 2.54*10^4/T-1.5*2.54-6.4$
upper andesite member	6.219×10^4	$\ln V = 2.74*10^4/T-1.5*2.74-6.4$
Pinabetoso Peaks basalt	6.130×10^3	$\ln V = 2.38*10^4/T-1.5*2.38-6.4$
Ute Mountain	4.395×10^5	$\ln V = 3.05*10^4/T-1.5*3.05-6.4$
Cerro de la Olla	6.536×10^4	$\ln V = 2.75*10^4/T-1.5*2.75-6.4$

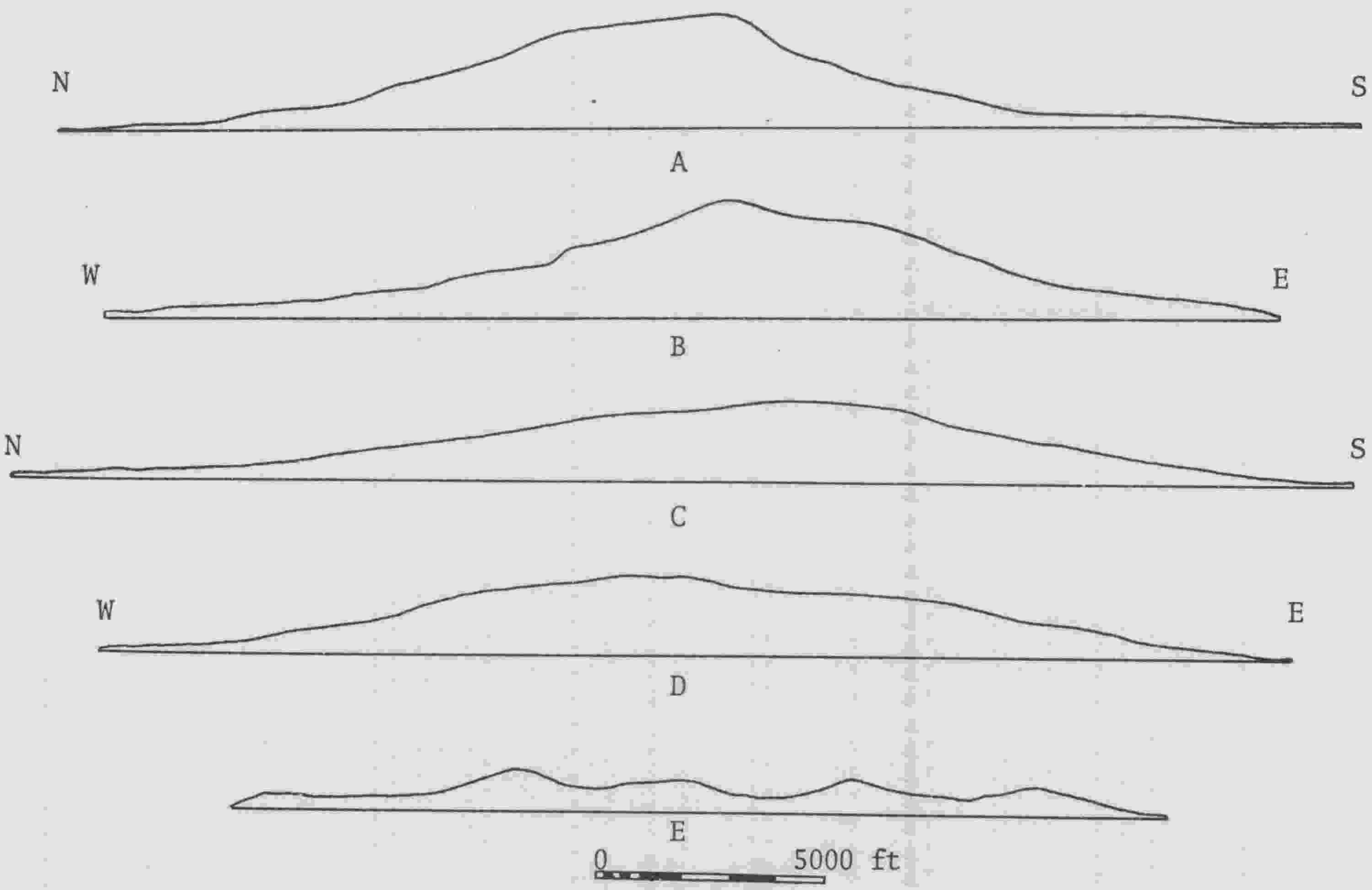

Figure 27. Profiles of volcanos in the Rio Grande Rift near San Antonio Mountain. A and B = Ute Mountain, C and D = Cerro de la Olla, E = No Agua Mountain.

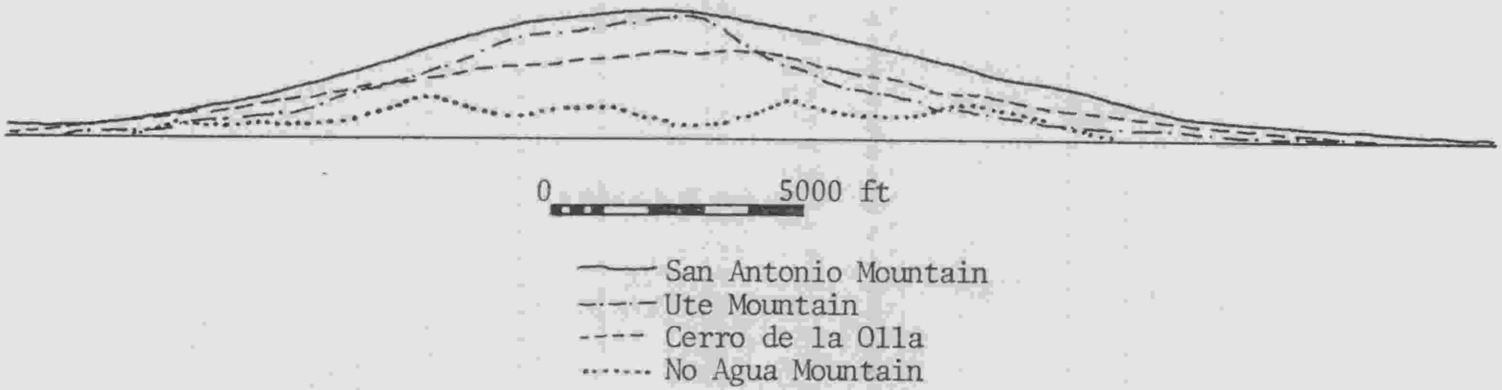

Figure 28. Constant scale comparisons of profiles of San Antonio Mountain, Cerro de la Olla, Ute Mountain and No Agua Mountain.

eruptions will increase the width of the structure with no increase in height, giving lower aspect ratios. Pyroclastic activity may steepen the sides of the volcano and increase the height, giving higher maximum slope angles and higher aspect ratios.

Tholeiite shields will have low profiles due to the low viscosity of the lavas. Pyroclastic activity will probably not affect the aspect ratio due to the great width of the shield relative to its height.

The morphology of the smaller lava and cinder cones will be more affected by eruptive history than bulk chemical composition. In addition to the factors mentioned earlier, the effects of explosion breaching will also affect the final morphology of the cone.

Flow Structures Within Latite Flows

Flow structures within individual latite flows are extremely varied. The structures are joints which developed during flow. A schematic diagram of an individual latite flow showing the orientation of joint surfaces is in Figure 30. The lava appears to have been solid enough to transmit the stress which formed the joints, but numerous grooves on joint surfaces (Fig. 29) indicate that the lava was still plastic during their formation. Within the interior of the flow, joint surfaces appear to be parallel to the base of the flow. Along the edges of the flow, joint surfaces rotate toward vertical, dipping in to the center.

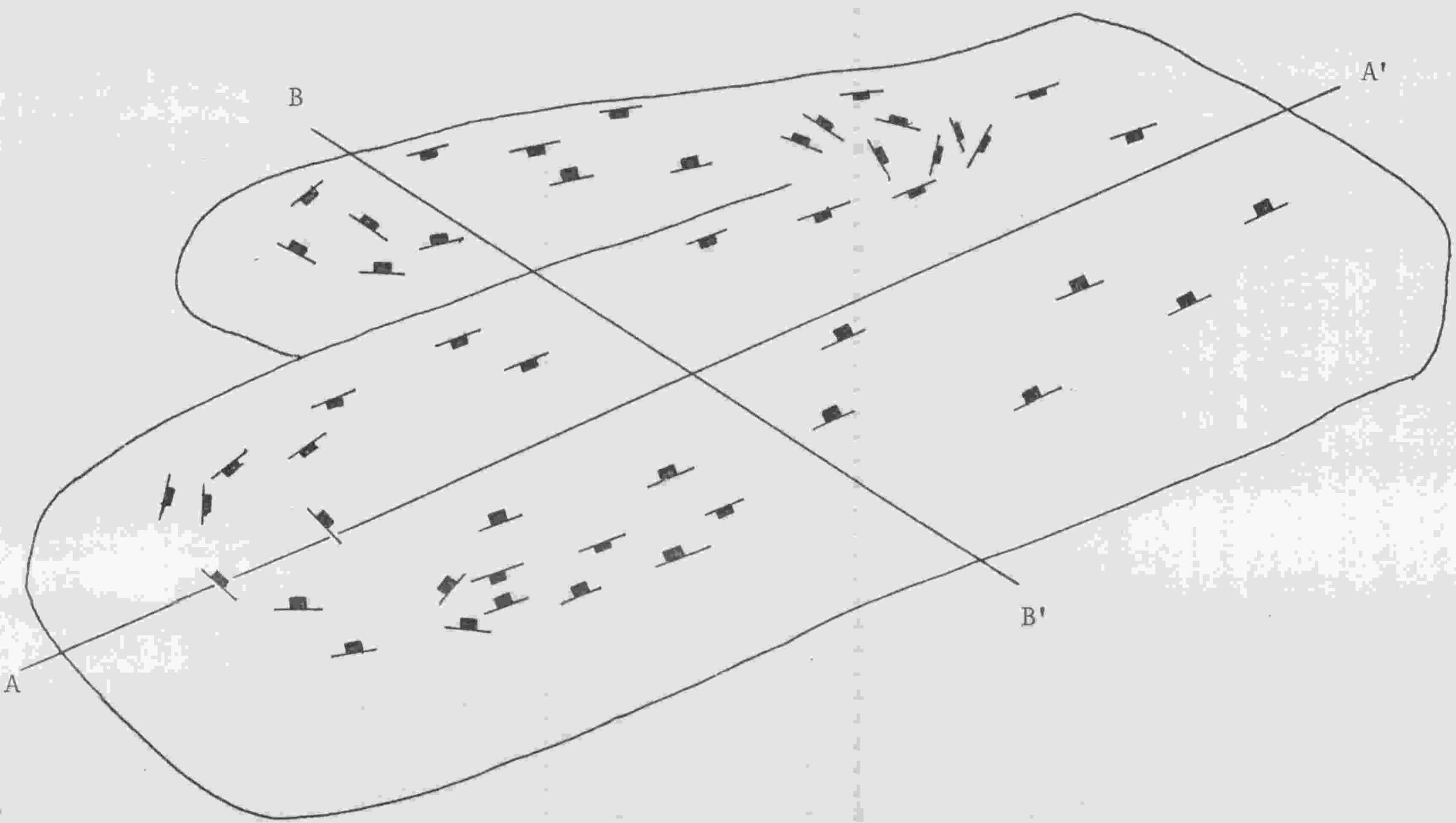

Figure 29a. Schematic drawing of a latite flow showing orientation of joint surfaces.

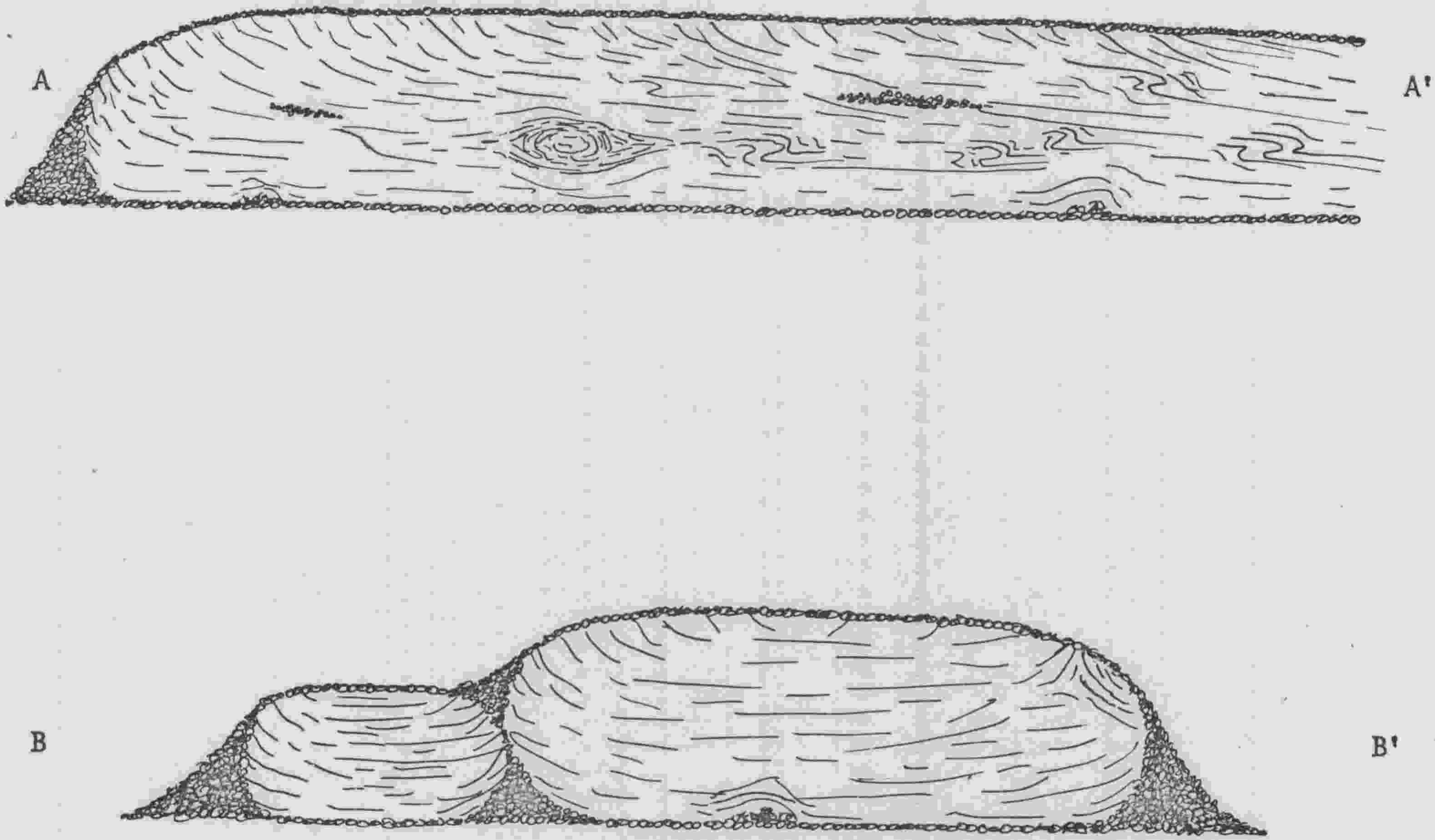

Figure 29b. Schematic longitudinal and transverse cross sections of a latite flow showing the orientation of joints.

Figure 30. Grooved joint surfaces of a latite flow from San Antonio Mountain, indicating movement of the flow while the lava was partially solid.

a

b

Figure 31. Flow structures in latite flows. a. Z-fold, amplitude 2 m. b. Synformal structure on the upper edge of a flow.

Figure 31c. "Augen" structure.

The upper surfaces of flows have rare synformal structures (Fig. 31b) and numerous tight, recumbent "z" folds are seen (Fig. 31a). The joints appear to have formed from shearing due to differing internal velocities. "Augen" structures (Fig. 31c) may be formed when the flow rotates an included block of latite during emplacement. Although joint surfaces are formed throughout the flow, they are developed best in the platy subunit (Fig. 9).

SUMMARY AND CONCLUSIONS

The San Antonio Mountain field area is a late Tertiary to early Quaternary volcanic terrane which is located along the southwestern edge of the San Luis Basin in the Rio Grande depression. Volcanism began with the eruption of the Wissmath Craters basalt, which built the shield volcano in the southeastern quadrant of the field area. Parts of the volcano were covered by basalt flows of the Servilletta Formation (Butler, 1946) which were erupted throughout the San Luis Basin 3.6-4.5 m.y. ago (Ozima _et al._, 1967). The basaltic andesite of Malette Creek was emplaced south of San Antonio Mountain some time after the eruption of the Servilletta Basalt. The location of the vents for this unit are unknown. The initial formation of the San Antonio Mountain volcanic complex began with the eruption of the first lower andesite member, which overlies the Malette Creek basalt. The basaltic andesites and lava cones of Red Hill and Los Cerritos de la Cruz were erupted after the emplacement of the first lower andesite member. Development of the San Antonio Mountain volcanic complex continued with the eruption of the second lower andesite member, which was overlain by the latite flow member. This unit has been dated at 3.04 ± 0.17 m.y. (P. W. Lipman, personal communication, 1975). The two lower andesite members and the latite flow member form the flow dome of San Antonio Mountain. The upper basaltic andesite member was erupted on the northeast flank of the mountain at 2.19 ± 0.15 m.y. (P. W. Lipman, personal communication, 1975). This was followed by the eruption of the upper andesite member. Finally, the basalt of the Piñabetoso Peaks was erupted east of San Antonio Mountain at 1.80 ± 0.72 m.y. (P. W. Lipman, personal communication, 1975) building interlayered cinder and lava cones over its vent.

Chemical data suggest that the volcanic rocks of the field area were derived from two magmas. One was olivine tholeiitic in composition and erupted the Servilletta Basalt. The location of the vents for the Servilletta Formation is not known, but they may be located east of the field area in the central portion of the San Luis Basin. The second magma erupted the other volcanic rocks of the field area and was calc-alkalic in composition. Three separate bodies of magmas were segregated from this magma and were emplaced beneath the field area at different locations, where they evolved independently to produce three series of rocks. One produced the basalts of Wissmath Craters, and the basaltic andesites of Malette Creek, Red Hill and Los Cerritos de la Cruz. The second magma erupted the lower andesite members and the latite flow member of the San Antonio Mountain volcanic complex. Chemical evolution of the third magma formed the upper basaltic andesite and andesite of San Antonio Mountain. The evolution of these magmas may have seen the result of fractionation, crustal contamination or both.

The volcanos of the field area can be divided into four morphologic groups. Cones built of interlayered lava and pyroclastics (north and south Piñabetoso Peaks) were formed when cinders are intruded by later lavas. The lavas dip in toward a central vent which is also probably the source of the pyroclastics. These cones have aspect ratios ~0.05-0.07. Lava cones (north and south Cerritos de la Cruz, Red Hill) are composed of lava flows which have piled up around a central vent and have steep, quaquaversal dips. Occasionally, some flows dip in toward the vent, forming a central amphitheater. These cones have maximum slope angles of 21°-31° and aspect ratios of 0.09-0.15. Some lava cones have been breached by later explosions. Shield volcanos (Wissmath Craters) are built of thin lava flows with low dip angles. Maximum slope angles are ~5° and aspect ratios (height/width) are ~0.02. Flow domes (San Antonio Mountain) are constructed of thick lava flows which have piled up around a central vent to form a steep domical structure. These volcanos have aspect ratios ~0.1 and maximum slope angles of 16°-19°.

Correlation of bulk chemical composition to external morphology indicates that for larger structures, such as flow domes and shield volcanos, chemical composition is the major factor in determining the morphology of the volcano. With increasing silica content, flows are thicker, more viscous and travel only a short distance from the vent, forming steep sided structures. Smaller structures, such as lava cones, are more dependant on eruptive history and vent conditions during eruption for their external morphology.

REFERENCES CITED

Aoki, K., 1967, Petrography and petrochemistry of latest Pliocene olivine tholeiites in the Taos area, northern New Mexico, U.S.A.: Contr. Mineral. and Petrol., v. 14, p. 190-203.

Bingler, E., 1968, Geology and mineral resources of Rio Arriba County, New Mexico: N. M. Bur. Mines and Min. Res. Bull. 91, 158 p.

Bowen, N. L., 1928, The evolution of the igneous rocks: Princeton, N. Y., Princeton Univ. Press, 332 p.

Bryan, K., 1938, Geology and groundwater conditions of the Rio Grande Depression in Colorado and New Mexico, in Regional Planning, pt. 6, Upper Rio Grande: Washington, Natl. Resources Comm., v. 1, pt. 2, sec. 1, p. 197-225.

Butler, A. P., 1946, Tertiary and Quaternary geology of the Tusas-Tres Piedras area, New Mexico: Harvard Univ., Cambridge, Mass., Ph.D. Dissert., 188 p.

____________, 1971, Tertiary volcanic stratigraphy of the eastern Tusas Mountains, southwest San Luis Valley, Colorado-New Mexico, in New Mexico Geol. Soc. Guidebook, 22nd Field Conf., p. 280-300.

Chapin, C., 1971, The Rio Grande Rift, Part 1: Modifications and additions, in New Mexico Geol. Soc. Guidebook, 22nd Field Conf., p. 191-201.

Francis, P., and Thorpe, R., 1974, Significance of lithologic and morphologic variations of pyroclastic cones: Geol. Soc. America Bull., v. 85, p. 927-930.

Funnell, B. M., 1964, The Tertiary Period, in The Phanerozoic time scale: suppl. to Quart. Jour. Geol. Soc. London, v. 120s, p. 179-191.

Heiken, G. H., 1971, Tuff rings: examples from the Fort Rock-Christmas Lake Valley basin, south central Oregon: Jour. Geophys. Res., v. 76, p. 5615-5625.

Higgins, M. W., 1973, Petrology of Newberry Volcano, central Oregon: Geol. Soc. America Bull., v. 84, p. 455-488.

Howe, E., 1909, Landslides in the San Juan Mountains, Colorado: U. S. Geol. Surv. Prof. Paper 67, 58 p.

Kelley, V. C., 1956, The Rio Grande Depression from Taos to Santa Fe, in New Mexico Geol. Soc. Guidebook, 7th Field Conf., p. 109-114.

____________, 1974, Albuquerque: Its mountains, rivers, valleys, water, and volcanos: Scenic trips to the geologic past, number 9: N. M. Bur. Mines and Min. Res., Socorro, N. M., 104 p.

Lambert, W., 1966, Notes on the Cenozoic geology of the Taos-Questa area, New Mexico, in New Mexico Geol. Soc. Guidebook, 17th Field Conf., p. 43-50.

Lipman, P. W., 1969, Alkalic and tholeiitic basaltic volcanism as related to the Rio Grande Depression, southern Colorado and northern New Mexico: Geol. Soc. America Bull., v. 80, p. 1343-1354.

___________, and Mehnert, H. H., 1975, Late Cenozoic basaltic volcanism and the development of the Rio Grande Depression in the southern Rocky Mountains: Geol. Soc. America Mem. 144, p. 119-154.

MacDonald, G. A., 1953, Pahoehoe, aa, and block lava: Am. Jour. Am. Jour. Sci., v. 251, p. 169-191.

___________, and Katsura, T., 1964, Chemical Composition of Hawaiian lavas: Jour. Petrology, v. 5, pt. 1, p. 82-133.

McGetchin, T. R., and Head, J. W., 1972, Lunar cinder cones: Science, v. 180, p. 168-170.

___________, Settle, M., and Chouet, B. A., 1974, Cinder cone growth modeled after Northeast Crater, Mt Etna, Sicily: Jour. Geophys. Res., v. 79, p. 3257-3272.

Montgomery, A., 1953, Precambrian geology of the Picuris range, north central New Mexico: N. Mex. State Bur. Mines and Min. Res. Bull. 30, 89 p.

Muehlberger, W. R., 1968, Geology of the Brazos Peak quadrangle, New Mexico: New Mex. State Bur. Mines and Min. Res. Geol. Map 22.

Naert, K. A., 1974, Geology, extrusion history, and analysis of perlites from No Agua, New Mexico: Penn. State Univ., State College, Penn., unpub. Ph.D. Dissert., 223 p.

Ozima, M., Kono, M., Kaneoka, I., Kinoshita, H., Kobayashi, K., Nagata, T., Larson, E., and Strangway, D., 1967, Paleomagnetism and K-Ar dates for some volcanic rocks of the Rio Grande Gorge, New Mexico: Jour. Geophys. Res., v. 72, no. 10, p. 2615-2621.

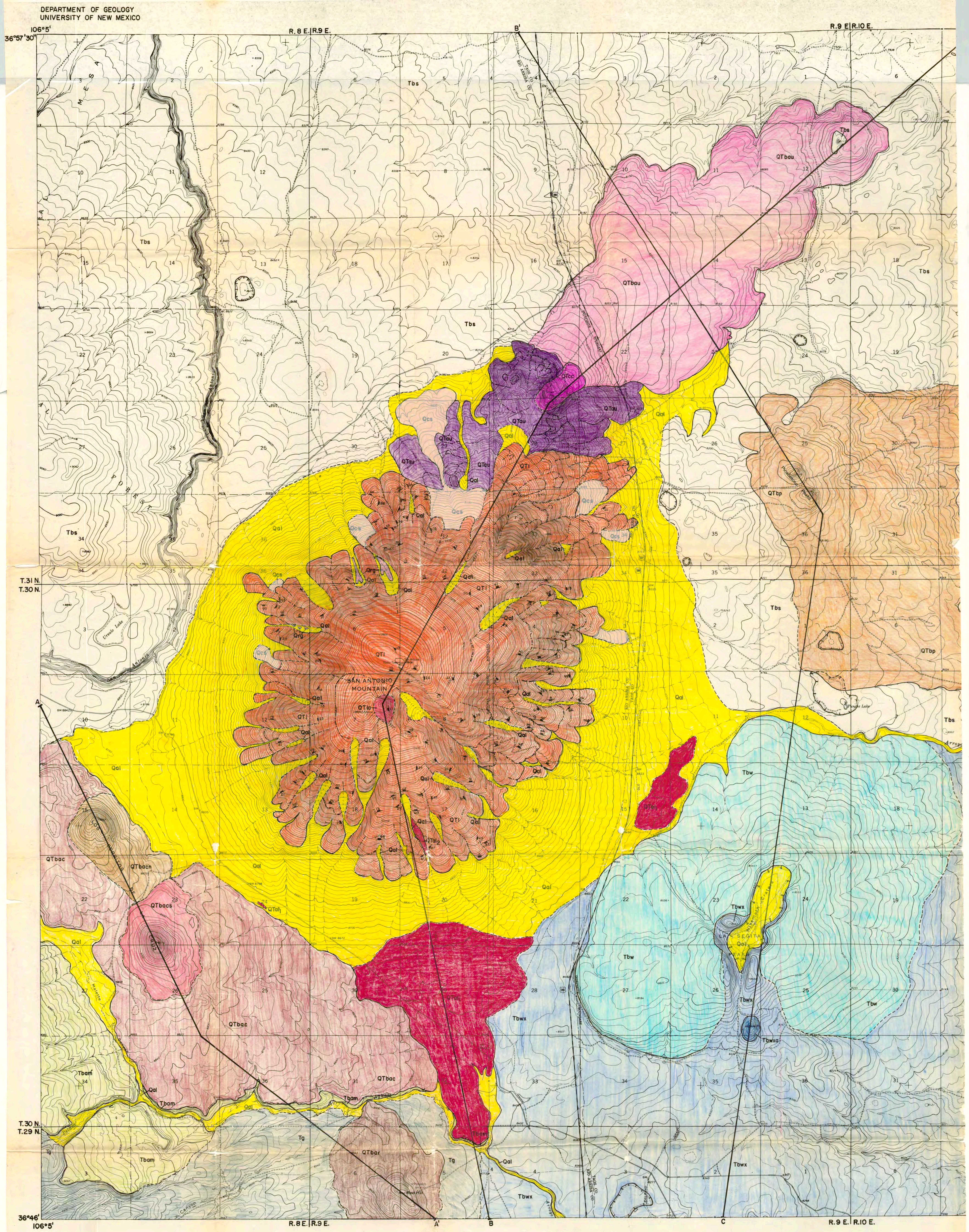

FIGURE IA.

GEOLOGIC MAP OF THE SAN ANTONIO MOUNTAIN AREA, TAOS AND ARRIBA COUNTIES, NEW MEXICO

D. EPPLER, 1976

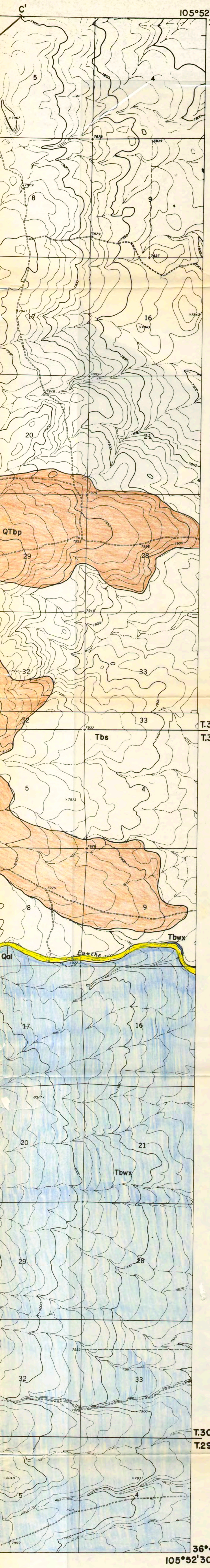

EXPLANATION

CORRELATION OF MAP UNITS

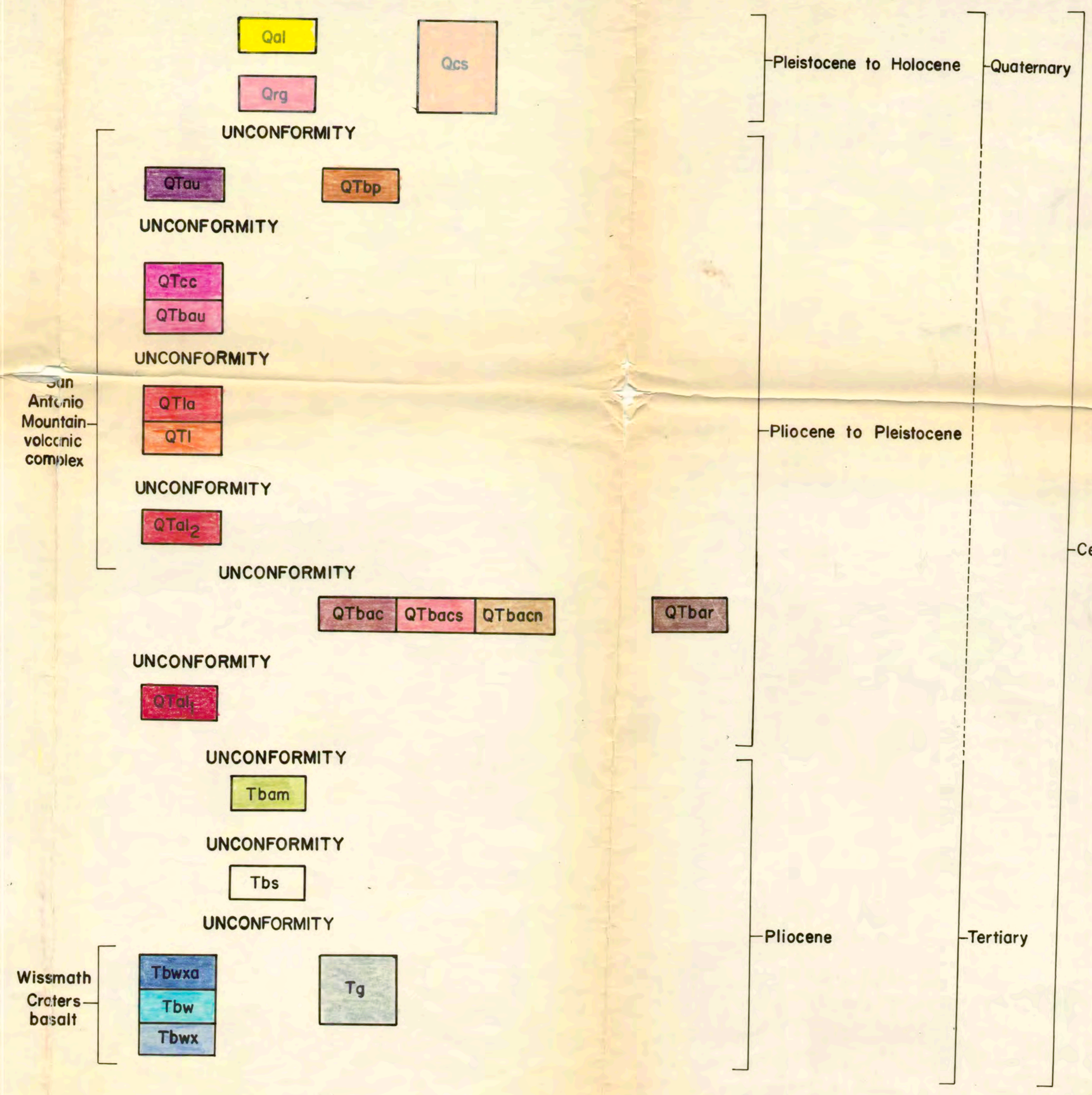

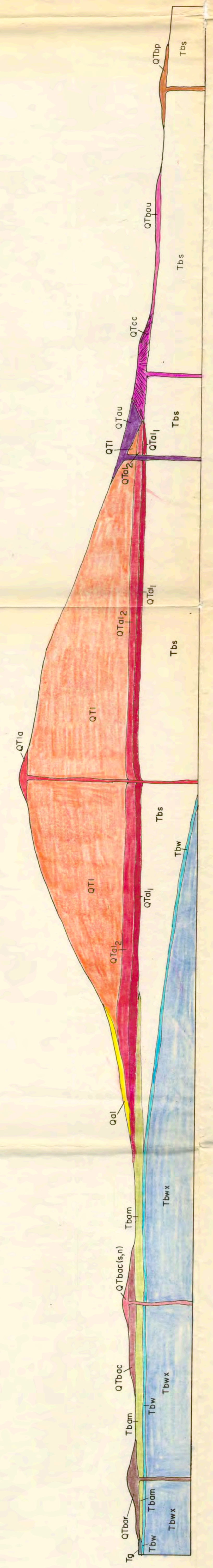

SCHEMATIC NORTH-SOUTH GEOLOGIC CROSS SECTION SHOWING FIELD RELATIONS BETWEEN MAP UNITS

DESCRIPTION OF MAP UNITS

Qal — ALLUVIUM- UNCONSOLIDATED SILT, SAND AND GRAVEL

Qcs — COLLUVIUM- UNCONSOLIDATED SILT, SAND AND GRAVEL DEPOSITED BY SOLIFLUCTION

Qrg — ROCK GLACIER DEPOSITS- UNCONSOLIDATED GRAVEL FOUND IN GLACIER-LIKE MASSES ON THE NORTHERN SLOPES OF SAN ANTONIO MOUNTAIN

QTbp — BASALT OF PINABETOSO PEAKS- FLOWBANDED OR PORPHYRITIC, INTERGRANULAR; MEGACRYSTS OF PARTIALLY RESORBED PLAGIOCLASE; PHENOCRYSTS OF AUGITE, HYPERSTHENE, OLIVINE AND PLAGIOCLASE; GROUNDMASS OF AUGITE, PLAGIOCLASE AND OPAQUE MINERALS. K-AR DATE 1.80 ± 0.72 M.Y. (P.W. LIPMAN, PERSONAL COMMUNICATION, 1975)

SAN ANTONIO MOUNTAIN VOLCANIC COMPLEX

QTau — UPPER ANDESITE MEMBER- VESICULAR, INTERSERTAL; RARE MEGACRYSTS OF PARTIALLY RESORBED PLAGIOCLASE; PHENOCRYSTS OF HYPERSTHENE; GROUNDMASS OF AUGITE, HYPERSTHENE, PLAGIOCLASE AND OPAQUE MINERALS IN A MESOSTASIS OF BROWN GLASS

QTcc — CINDER CONE MEMBER- UNCONSOLIDATED ASH, LAPILLI AND BLOCKS UP TO 50 CM; SPARSE QUARTZ XENOCRYSTS; COMPOSITION PROBABLY BASALTIC ANDESITE

QTbau — UPPER BASALTIC ANDESITE MEMBER- VUGGY, INTERSERTAL; ABUNDANT XENOCRYSTS OF QUARTZ; SPARSE MEGACRYSTS OF PARTIALLY RESORBED PLAGIOCLASE; PHENOCRYSTS OF HYPERSTHENE; GROUNDMASS OF AUGITE, HYPERSTHENE, PLAGIOCLASE AND OPAQUE MINERALS IN A GLASSY TO DEVITRIFIED MESOSTASIS. K-AR DATE 2.18 M.Y. (P.W. LIPMAN, PERSONAL COMMUNICATION, 1975)

QTla — LATITE AGGLOMERATE MEMBER- ANGULAR FRAGMENTS OF GLASSY LATITE IN A MESOSTASIS OF PLAGIOCLASE MICROLITES AND RED GLASS

QTl — LATITE FLOW MEMBER- PORPHYRITIC, BLACK, GLASSY AND MASSIVE TO SILVERY, HOLOCRYSTALLINE AND VESICULAR; PHENOCRYSTS OF HYPERSTHENE; GROUNDMASS OF AUGITE, PLAGIOCLASE AND OPAQUE MINERALS. K-AR DATE 3.04 ± 0.17 M.Y. (P.W. LIPMAN PERSONAL COMMUNICATION, 1975)

$QTal_2$ — SECOND LOWER ANDESITE MEMBER- VESICULAR, INTERSERTAL; GROUNDMASS OF AUGITE, HYPERSTHENE, PLAGIOCLASE AND OPAQUE MINERALS IN A BLACK GLASSY MESOSTASIS

$QTal_1$ — FIRST LOWER ANDESITE MEMBER- VESICULAR, INTERSERTAL; PHENOCRYSTS OF HYPERSTHENE, PLAGIOCLASE AND OLIVINE RIMMED BY PYROXENE; GROUNDMASS OF AUGITE, HYPERSTHENE, PLAGIOCLASE AND OPAQUE MINERALS

QTbac — BASALTIC ANDESITE OF LOS CERRITOS DE LA CRUZ- INTERGRANULAR; XENOCRYSTS OF QUARTZ, MEGACRYSTS OF PARTIALLY RESORBED PLAGIOCLASE; PHENOCRYSTS OF AUGITE, HYPERSTHENE AND PLAGIOCLASE; GLASSY GROUNDMASS OF INTERGROWN AUGITE PLAGIOCLASE, AND OPAQUE MINERALS. QTBACN- FLOWS ERUPTED FROM THE NORTHERN VENT; QTBACS- FLOWS ERUPTED FROM THE SOUTHERN VENT

QTbar — BASALTIC ANDESITE OF RED HILL- VESICULAR, INTERGRANULAR; PHENOCRYSTS OF AUGITE, HYPERSTHENE AND OLIVINE; GROUNDMASS OF AUGITE AND PLAGIOCLASE

Tbam — BASALTIC ANDESITE OF MALETTE CREEK- DIKTYTAXITIC; XENOCRYSTS OF QUARTZ; PHENOCRYSTS OF AUGITE, HYPERSTHENE, OLIVINE, AND PLAGIOCLASE; GROUNDMASS OF AUGITE AND OPAQUE MINERALS

Tbs — BASALT OF THE SERVILLETTA FORMATION (BUTLER, 1946; MONTGOMERY, 1953) DIKTYTAXITIC; OLIVINE AND PLAGIOCLASE POIKILITICALLY ENCLOSED IN AUGITE; FELTY MESOSTASIS OF AUGITE, PLAGIOCLASE AND OPAQUE MINERALS; K-AR DATE 3.66 ± 0.77 M.Y. (P.W. LIPMAN, PERSONAL COMMUNICATION, 1975)

Tg — GRAVEL- LOOSELY CONSOLIDATED SILT, SAND AND COBBLES DERIVED FROM PRECAMBRIAN GRANITIC PEGMATITE AND TERTIARY ASH FLOW TUFF

BASALT OF WISSMATH CRATERS

Tbwxa — XENOCRYSTIC ALKALI BASALT MEMBER- INTERSERTAL; XENOCRYSTS OF QUARTZ AND FUSED SEDIMENTS; PHENOCRYSTS OF AUGITE AND OLIVINE; GROUNDMASS OF PLAGIOCLASE AND OPAQUE MINERALS IN A MESOSTASIS OF BROWN GLASS.

Tbw — OLIVINE THOLEIITE MEMBER- INTERGRANULAR, PORPHYRITIC; PHENOCRYSTS OF AUGITE, OLIVINE AND PLAGIOCLASE; GROUNDMASS OF AUGITE, PLAGIOCLASE AND OPAQUE MINERALS

Tbwx — XENOCRYSTIC THOLEIITE MEMBER- INTERGRANULAR, PORPHYRITIC; XENOCRYSTS OF PYROXENE-RIMMED QUARTZ; MEGACRYSTS OF PARTIALLY RESORBED PLAGIOCLASE; GROUNDMASS OF AUGITE, OLIVINE AND PLAGIOCLASE

SYMBOLS

- contact, dashed where approximate
- lava flow boundary, dotted where buried
- fault, ball on downthrown side
- flow joint
- collapse pit

LOCATION MAP

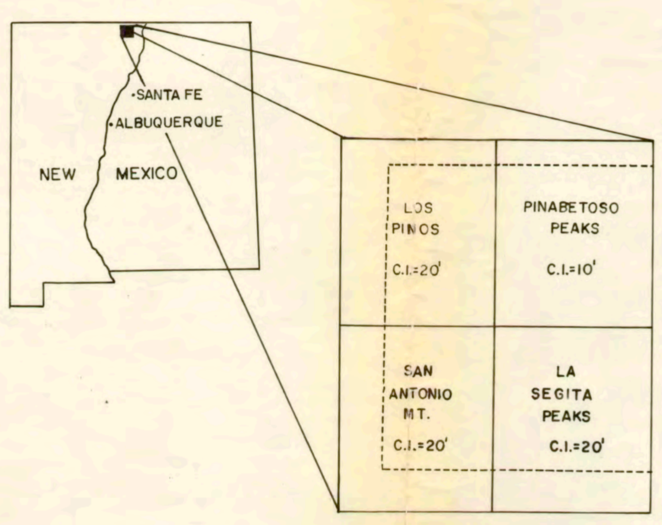

SCALE

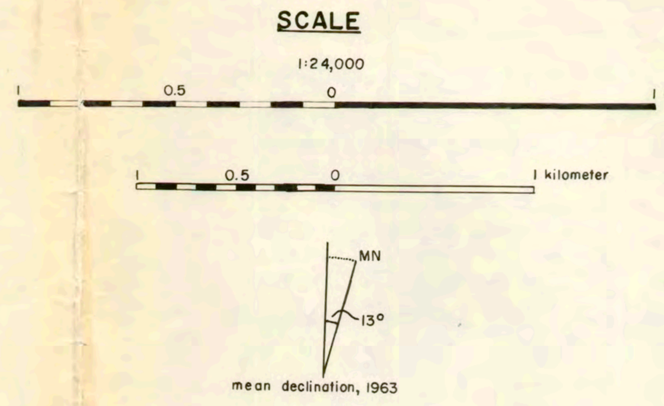

DEPARTMENT OF GEOLOGY
UNIVERSITY OF NEW MEXICO

FIGURE IC. MORPHOLOGIC CROSS SECTIONS

DEPARTMENT OF GEOLOGY
UNIVERSITY OF NEW MEXICO

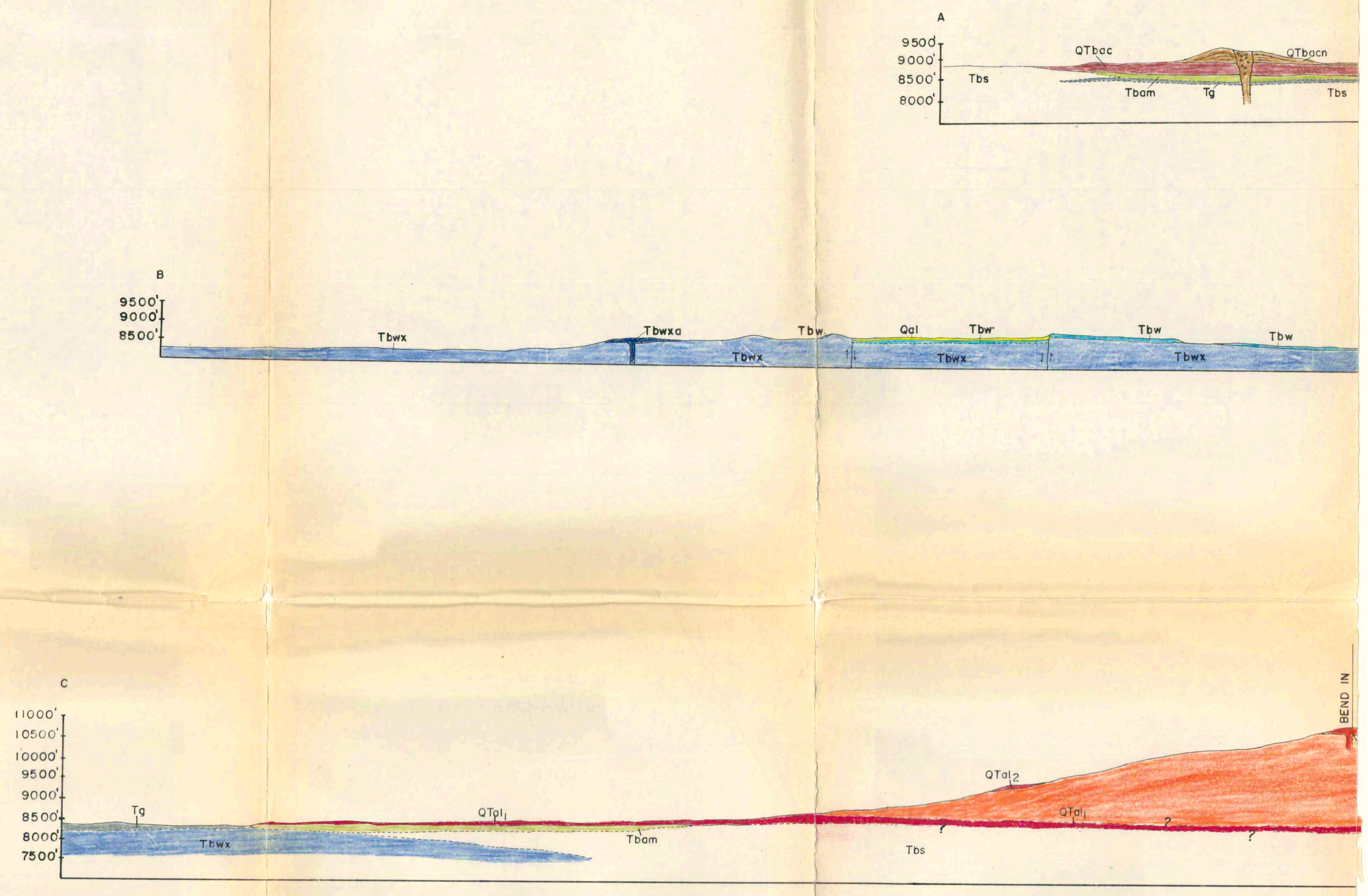

GEOL

FIGURE IB.

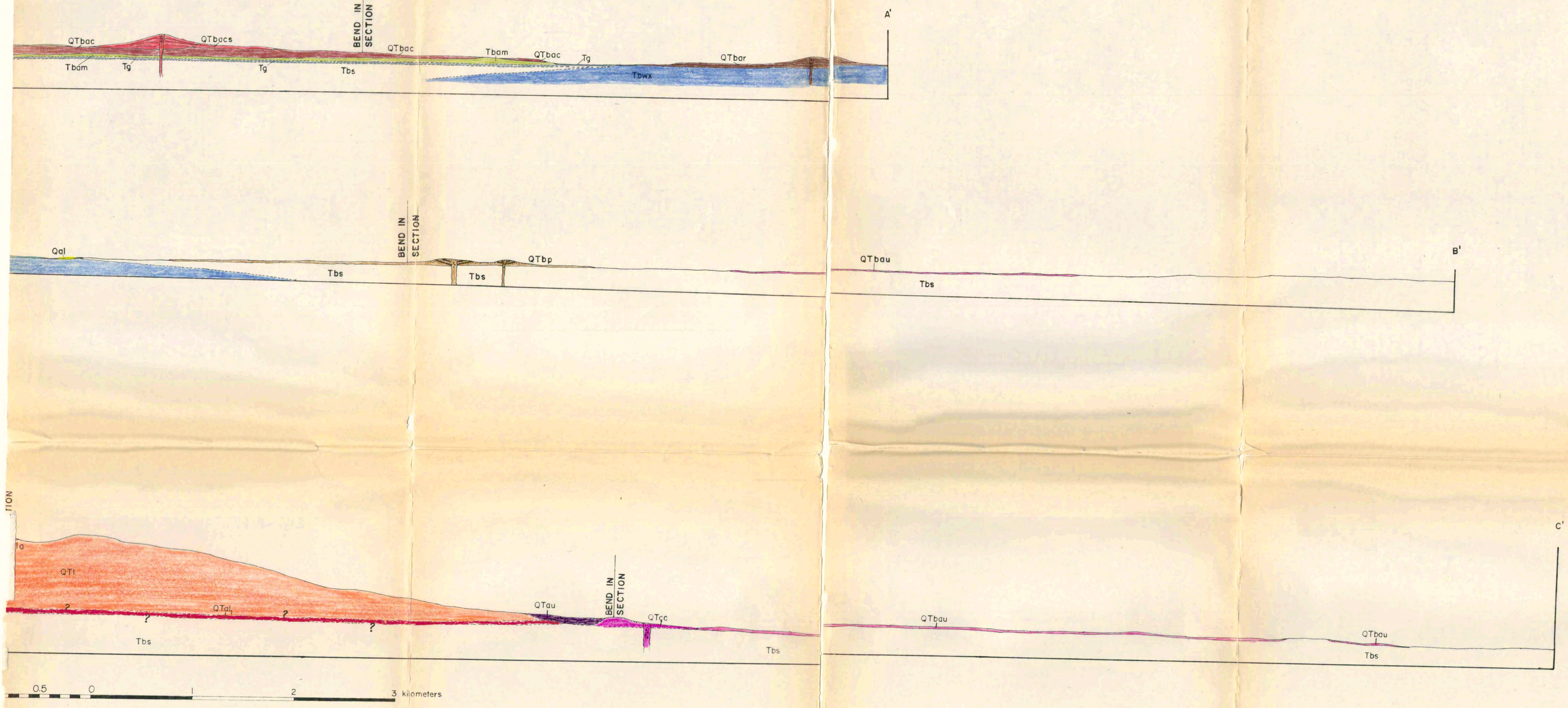

FIGURE IB.

...OGIC CROSS SECTIONS, SAN ANTONIO MOUNTAIN AREA

TAOS AND RIO ARRIBA COUNTIES, NEW MEXICO

explanation of symbols and location of cross sections on Figure IA.